

# Interior Climate U-Value calculation and optimization for electric buses at Volvo buses

Master's thesis in Master's program Sustainable Energy Systems

HAMIDREZA SAHRAEI



MASTER'S THESIS IN PROGRAMME Sustainable Energy Systems

# Interior Climate U-Value calculation and optimization for electric buses at Volvo buses

HAMIDREZA SAHRAEI



Department of Mechanics and Maritime Sciences  
Division of Vehicle Engineering and Autonomous Systems (VEAS)

CHALMERS UNIVERSITY OF TECHNOLOGY  
Göteborg, Sweden 2020

Interior Climate U-Value calculation and optimization for electric buses at Volvo buses

HAMIDREZA SAHRAEI

© HAMIDREZA SAHRAEI, 2020

Master's Thesis 2020:39

Department of Mechanics and Maritime Sciences

Division of Vehicle Engineering and Autonomous Systems (VEAS)

Supervisors: Ronnie Malm, Volvo Buses

Christoph Boettcher, Gamma Technologies

Examiner and supervisor at Chalmers: Jelena Andric, Division of Vehicle Engineering and Autonomous System

Chalmers University of Technology

SE-412 96 Göteborg

Sweden

Telephone: + 46 (0)31-772 1000

Cover: Customized Cabin model for electric buses in GT-SUITE

Chalmers Reproservice / Department of Mechanics and Maritime Sciences  
Göteborg, Sweden 2020-01-01

## Interior Climate U-Value calculation and optimization for electric buses at Volvo buses

Master's thesis in Sustainable Energy Systems

HAMIDREZA SAHRAEI

Department of Mechanics and Maritime Sciences

Division of Vehicle Engineering and Autonomous Systems (VEAS)

Chalmers University of Technology

### Abstract

Improving energy efficiency while complying with the interior climate requirements is one of the main challenges in electric buses. Heat Ventilation and Air Conditioning (HVAC) system of electric buses has a rather large share of total energy consumption during driving. Compared to conventional buses that use internal combustion engines, there is less excess heat from an electric motor in electric buses. Therefore, improving the HVAC system's energy efficiency can increase the driving range of electric buses. In this master thesis calculation of the U-value for the Volvo electric bus was performed using the GT-SUITE simulation software. The suggestions for improving the energy efficiency of the Volvo electric bus were discussed as well.

Key words: Electric Buses, HVAC, U-Value, Interior Climate, Energy Simulation, GT-SUITE

# Contents

Abstract .....	1
Contents .....	2
Preface .....	6
Acknowledgements .....	6
Notations.....	7
1 Introduction .....	8
1.1 Background.....	8
1.2 Objectives .....	8
1.3 Limitations and assumptions .....	8
1.4 Ethical aspects of research .....	8
2 Theory.....	9
2.1 Heat transfer theory.....	9
2.1.1 Heat conduction .....	9
2.1.2 Heat convection.....	10
2.1.3 Radiation .....	10
2.2 Heat Balance Method (General) .....	11
2.2.1 Elements in HBM.....	11
2.3 Heat Balance Method (HBM) for vehicles .....	12
2.3.1 Net overall thermal load ( $Q_{Tot}$ ).....	12
2.3.2 Metabolic Load ( $Q_{Met}$ ) .....	13
2.3.3 Radiation Loads ( $Q_{Dir}$ , $Q_{Dif}$ , $Q_{Ref}$ ).....	13
2.3.4 Ambient load ( $Q_{Amb}$ ).....	13
2.3.5 Ventilation Load ( $Q_{ven}$ ).....	14
2.3.6 Exhaust load ( $Q_{Exh}$ ) .....	14
2.3.7 Engine load ( $Q_{Eng}$ ).....	14
2.3.8 AC loads ( $Q_{ven}$ ) .....	14
2.4 U-value calculation methods .....	15
2.4.1 U-value calculation estimated method .....	15
3 Methodology.....	16
3.1 HVAC system Components .....	16
3.2 Heat balance method (HBM) for an electric bus .....	17
3.3 Simulation using GT-SUITE .....	17
3.3.1 Proper model selection in GT-SUITE .....	17
3.3.2 Required input for modelling .....	17
3.3.3 Material definition based on the CAD model.....	18
2 <b>CHALMERS</b> , <i>Mechanics and Maritime Sciences</i> , Master's Thesis 2020:39	

3.3.4	Calculation of the equivalent U-VALUE for each surface.....	18
3.3.5	Average U-Value Calculation of the cabin.....	19
3.3.6	Defining average specific heat, density and weight of the elements.....	19
3.3.7	Defining internal heat gains .....	19
3.3.8	Defining parameters for thermal comfort prediction .....	19
3.3.9	Defining initial conditions.....	19
3.3.10	Calibration of the model .....	19
3.4	Improving U-Value of the bus's body .....	24
3.4.1	Increasing the material thicknesses .....	24
3.4.2	Adding new materials .....	24
3.4.3	Replacing the materials using Ashby bubble plots .....	24
4	Results and discussion.....	27
4.1	Calibration model results.....	27
4.1.1	Results categories.....	27
4.2	Calculation of the U-Value with different approaches .....	32
4.2.1	U-Value calculation based on the estimated method by defining the HTCs based on the standards.....	32
4.2.2	U-Value calculation based on the estimated method using HTCs from GT-SUITE results.....	32
4.2.3	U-Value calculation based on the heat rates from GT-SUITE results .....	32
4.2.4	Comparison between U-Values from different approaches.....	32
4.3	Suggestions for improving the model's accuracy.....	33
4.3.1	Calibration the model for a transient model.....	33
4.3.2	Using multi-zone model.....	33
4.3.3	Adding HVAC equipment to the model.....	33
4.3.4	Applying door opening schedules.....	34
4.4	Comparison between estimated U-Values and infrared photos.....	34
4.5	Suggestions for improving the U-Value of the bus's body.....	35
4.5.1	Increasing the material thicknesses .....	35
4.5.2	Adding new materials .....	35
4.5.3	Replacement of the materials using Ashby bubble plots .....	36
4.5.4	Studying the effect of replacing plywood with one of the alternatives.....	38
4.5.5	Replacement of the side windows.....	39
5	Conclusions.....	40
6	References.....	41

## List of figures

Figure 2-1 The range of thermal conductivity for different materials (CES results) .....	9
Figure 2-2 Different trend for variation of the thermal conductivity with temperature for two material types .....	10
Figure 2-3 ASHRAE Heat Balance Method showing a nodal network for a wall with the outside surface on the left .....	11
Figure 2-4 Heat balance process in a zone based on ASHRAE HBM .....	12
Figure 2-5 CEB tool for thermal comfort prediction.....	15
Figure 3-1 HVAC components in the electric bus. 1, 2 and 3 are the AC system, heat blowers, convectors and defroster, respectively.....	16
Figure 3-2 Heat balance method for an electric bus .....	17
Figure 3-3 Cabin calibration model in GT-SUITE .....	20
Figure 3-4 Position of six points where the experimental data is measured [10] .....	20
Figure 3-7 Results for two step calibration approach. Case 1 steady state calibration and case 2 transient calibration .....	21
Figure 3-8 An example of the realistic heat rate for the heating system.....	22
Figure 3-9 Simulation results for a case with a manual heat rate .....	22
Figure 3-10 Simulation results for a case with PID controller .....	23
Figure 3-11 Comparison between density and thermal conductivity of different material groups with plywood (CES Results) .....	25
Figure 3-12 Comparison between the conductivity and young modulus of different material groups with plywood.....	25
Figure 3-13 Elastic bending condition in floor part.....	26
Figure 4-1 Simulation results for the calibrated model.....	27
Figure 4-2 Cabin pressure change trend with changing the temperature.....	28
Figure 4-3 Comparison between cabin air temperature and cabin mass temperature....	28
Figure 4-4 Roof insulation temperature trend during the simulation in different parts, inside, outside and center .....	29
Figure 4-5 Calculation of U-Value for bus's part based on the heat rate results from GT-SUITE .....	29
Figure 4-6- A CFD results shows temperature distribution for a similar case.....	30
Figure 4-7 CFD results that shows temperature distribution in a steady state case.....	30
Figure 4-8 PPD result during the simulation time .....	31
Figure 4-9 PVM result during the simulation time.....	31
Figure 4-10 U-Value calculation based on the heat rates for different parts of the bus .....	32
Figure 4-11 Comparison between U-Value calculation results from three different approaches .....	33
Figure 4-12 Cabin model integration with HVAC system (GT-SUITE tutorials).....	34
Figure 4-13 Areas with higher U-Values based on the calculation .....	35
Figure 4-14 Ashby plot for Young modulus vs Thermal conductivity.....	36
Figure 4-15 Ashby bubble plot for Young modulus vs density times cost per kilogram .....	37

## List of tables

Table 3-1 Estimation approach for setting the parameters – General input.....	18
Table 3-2 Estimation approach for setting of parameters –thermal comfort.....	19
Table 3-3 PID controller setting in GT-SUITE.....	23
Table 3-4 Settings for GT-SUITE Optimizer.....	23
Table 3-5 Problem translation for material selection of floor part.....	26
Table 4-1 Results for applying increasing material’s thickness strategy.....	35
Table 4-2 Results for applying adding insulation materials strategy.....	35
Table 4-3 Alternative materials suggested by CES after first stage.....	37
Table 4-4 Alternative materials suggested by CES software after second stage.....	38
Table 4-5 Results for applying material replacement strategy.....	38
Table 4-6 Results for side windows replacement.....	39

## **Preface**

This master's thesis has been performed during the spring of 2020 by Hamidreza Sahraei as a part of the master's program Sustainable Energy Systems at Chalmers University of Technology. The thesis was performed at Volvo Bus Corporation with supervision of Ronnie Malm (Principal Feature Leader Interior Climate at Volvo Buses) and Christoph Boettcher (Technical Consultant at Gamma Technologies GmbH). The thesis also was supervised and examined by Jelena Andric at Division of Vehicle Engineering and Autonomous Systems (VEAS) at Mechanics and Maritime Sciences department at Chalmers University of Technology.

Göteborg June 2020

HAMIDREZA SAHRAEI

## **Acknowledgements**

I would like to offer special gratitude to my industrial supervisors Ronnie Malm and Christoph Boettcher for their professional support during the thesis work especially during the critical situation due to the corona virus pandemic.

I would also like to have a special thanks to Jelena Andric for her professional guidance and support from the beginning to the end of the work. Without her kind support, it would not have been possible to get planned results because of the limitations in accessing the experimental data.

I also want to thank Majid Astaneh from the Division of Vehicle Engineering and Autonomous Systems (VEAS) for his help with learning the GT-SUITE and Negar Panahi from the Department of Materials Engineering who helped me for material selection part.

## Notations

### Abbreviations

HVAC	Heat, Ventilation, Air Condition
HTC	Heat Transfer Coefficient
HBM	Heat Balance Method
PPD	Population Percent Dissatisfied
PVM	Predicted Mean Vote

### Nomenclature

$T$	Time
$\lambda$	Thermal Conductivity
$h$	Heat transfer coefficient
U-Value	Thermal transmittance
$\rho$	Density
$c_p$	Specific heat constant
$T$	Temperature
$h$	Convection heat transfer coefficient
$q''$	Convective heat flux
$E$	Total energy
$Q$	Heat transfer
$\dot{m}$	Mass flow rate
$V$	Volume flow rate
$R$	Thermal resistance
$e_b$	Energy emission
$\sigma$	Stefan-Boltzmann constant
$F_{1-2}$	View Factor
$\varepsilon$	Emissivity
$f_{1-2}$	Transmission Factor

# 1 Introduction

## 1.1 Background

Volvo buses is working on improving energy efficiency and interior climate of electric buses. One of the main challenges in electric buses is their rather high energy demand for the HVAC (Heat Ventilation Air Conditioning) system. Compared to conventional buses that use internal combustion engines, there is less excess heat from electric motor in electric buses. In certain weather conditions, the electricity demand to fulfil the HVAC requirements is a large share of the total electricity consumption in an electric bus. While in conventional vehicles fuel economy is the most interesting factor, in electric vehicles, the goal can be defined as widening the range a vehicle can transport between each recharging or increasing driving range. Improving the energy efficiency of the electric bus will increase the driving range of the vehicle and decrease the size of batteries. In addition, due to the fact that batteries are heavy, this improvement may indirectly affect the engine power consumption of the electric buses.

## 1.2 Objectives

Optimal energy consumption and interior climate quality can be achieved by calculating the U-Value (Thermal Transmittance) for a vehicle. The lower U-Value achievement, the lower energy losses for a bus. This Master Thesis will investigate the possibilities of obtaining higher energy efficiencies from an interior climate point of view. The focus is to create energy model for an electric bus in GT-SUITE system level simulation software and perform full calculation of the U-Value based on the available 3D CAD model and relevant material properties. In addition, the sensitivity analysis will be performed to optimize energy consumption. Finally, some recommendations for improving the design of electric buses will be suggested.

## 1.3 Limitations and assumptions

For calculation and modelling of the bus, some limitations and in several cases realistic simplifications and assumptions have been considered.

The mass for the 1D HVAC system would be considered as a lumped mass. All equations will be solved in one dimension in GT-SUITE. Therefore, quantities are averages across the flow direction.

Some other assumptions can be listed as follows:

- Air gaps and related losses were considered to be a part of U-Value.
- Complicated cross-sectional profiles have been replaced by simplified geometries.
- A uniform surface temperature have been assumed.
- Long wave (LW) and short wave were considered to have uniform irradiations.
- All heat conductions will be assumed to be in one dimension

## 1.4 Ethical aspects of research

Improving the performance of electric buses will have a positive societal, ethical and ecological impact. It is obvious that improving the energy efficiency of electric buses and improving passenger's thermal comfort has direct effect on the development and promotion of this type of buses. Less local noise and air pollution will provide healthier residential areas. In case of producing electricity from the renewables, CO<sub>2</sub> emission could be significantly reduced when replacing diesel vehicles with electric ones.

## 2 Theory

Heat transfer theory, heat balance method and U-Value definition can be named as the foundations used in calculations and modelling of this project.

### 2.1 Heat transfer theory

Based on the heat transfer theory there are three mechanisms for transferring heat: Conduction, convection and radiation.

#### 2.1.1 Heat conduction

Conduction follows Fourier's law for one-dimensional heat conduction. For having thermal conduction, a temperature gradient inside the material is required. For instance, in x direction, the conduction heat flux ( $\dot{q}_{cond}$ ) for a local thermal gradient of  $\frac{\partial T}{\partial x}$  can be calculated as shown in equation 2-1.

$$\dot{q}_{cond} = -\lambda \frac{\partial T}{\partial x} \quad 2-1$$

The constant  $\lambda$  (also referred as "k" in some text books), is called thermal conductivity. The heat flux is a vector quantity and the negative sign means that the flux will flow from higher temperature side to lower temperature side. The three-dimensional form of the Fourier's law can be written as described in equation 2-2.

$$\vec{q} = -\lambda \nabla T \quad 2-2$$

##### 2.1.1.1 Thermal conductivity

The range of the thermal conductivity is different and varies by a factor of  $10^5$  between different materials. Figure 2-1 shows the approximate ranges of thermal conductivity of various substances [1].

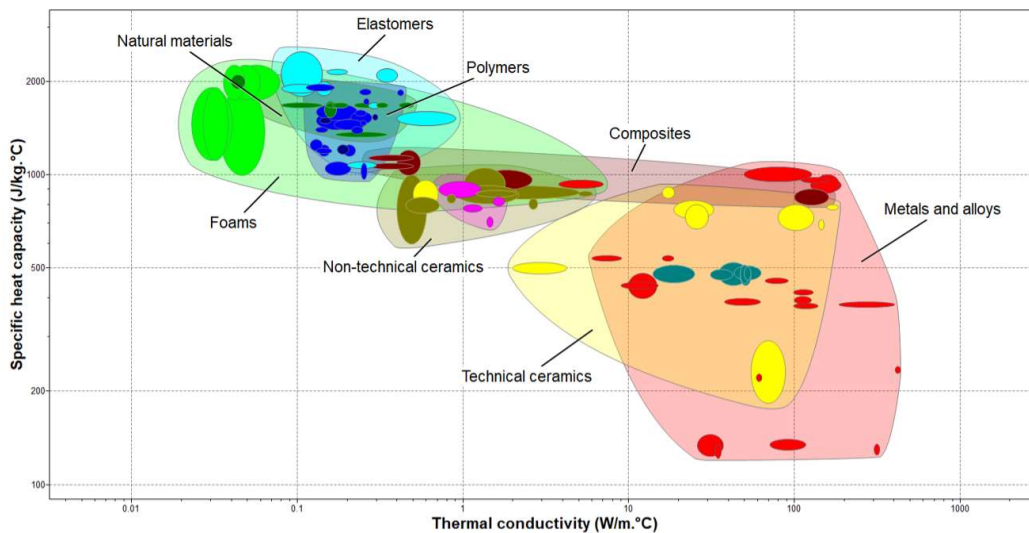


Figure 2-1 The range of thermal conductivity for different materials (CES results)

##### 2.1.1.2 Thermal conductivity variation with temperature

Thermal conductivity of materials changes with temperature. This change is significant for some materials while for some other materials the effect of the temperature on thermal

conductivity is negligible. Figure 2-2 shows the impact of changing temperature on thermal conductivity of Polyurethane and Aluminum.

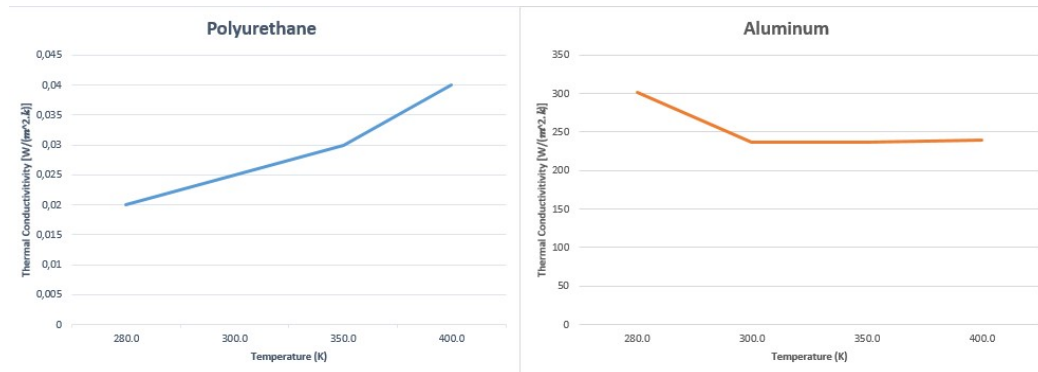


Figure 2-2 Different trend for variation of the thermal conductivity with temperature for two material types

### 2.1.2 Heat convection

For fluids, convection is another mechanism of heat transfer. The heat flux resulted from convection can be calculated as shown in equation 2-3. The constant  $\bar{h}$  in equation 2-3 is the heat transfer coefficient [1, p. 26].

$$q = \bar{h}(T_{body} - T_{\infty}) \quad 2-3$$

Convection could occur in two ways, natural convection and forced convection.

### 2.1.3 Radiation

The electromagnetic radiation is the third mechanism of heat transfer. In radiation, the radiant energy flux depends upon the temperature of the body and surface properties [1, p. 26]. Unlike the convection and conduction, radiation mechanism does not need a medium for transferring. Due to the lower amounts of radiation heat transfer in contrast with convection and conduction, in most cases, radiant heat transfer can be neglected for cold bodies. However, radiation could be a significant fraction of heat transfer when it occurs at high temperatures or in case of vacuum.

Based on the Stefan-Boltzmann law for a black body, this energy emission ( $e_b(T)$ ) can be calculated as described in equation 2-4, where  $\sigma$  is  $5.670374 \times 10^{-8} \frac{W}{m^2 \cdot K^4}$  and T is the absolute temperature [1, p. 30].

$$e_b(T) = \sigma T^4 \quad 2-4$$

Based on the Stefan-Boltzmann law, the radiation interaction between two bodies ( $Q_{net}$ ) with surface temperatures of  $T_1$  and  $T_2$  can be calculated as shown in equation 2-5. In equation 2-5,  $A_1$  represents the surface area between two bodies.

$$Q_{net} = A_1 e_b(T_1) - A_1 e_b(T_2) = A_1 \sigma (T_1^4 - T_2^4) \quad 2-5$$

Equation 2-5 calculates the net heat transferred from object 1 to object 2. As shown in equation 2-6, in case that object 1 sees another objects in addition to object 2, an extra term, so called view factor ( $F_{1-2}$ ) shall be added to the equation.

$$Q_{net} = A_1 F_{1-2} \sigma (T_1^4 - T_2^4) \quad 2-6$$

In addition, non-black bodies absorb and emit less radiation than black bodies. As shown in equation 2-7, the emissive power of a non-black body ( $e_{non-black}$ ), can be characterized using a property called emittance or emissivity ( $\epsilon$ ) [1, p. 33].

$$e_{non-black} = \epsilon e_b = \epsilon \sigma T^4 \quad 2-7$$

$$0 < \epsilon \leq 1$$

In a similar way as the black body formulation, for two non-black bodies, the net exchanged radiation can be written as shown in equation 2-8, where the transfer factor ( $f_{1-2}$ ) depends on the geometrical view and emittances of both bodies.

$$Q_{net} = A_1 f_{1-2} \sigma (T_1^4 - T_2^4) \quad 2-8$$

## 2.2 Heat Balance Method (General)

The Heat Balance Method (HBM) is a common method for calculation of heating and cooling loads in a space or zone suggested by ASHRAE (American Society of Heating, Refrigerating and Air-Conditioning). Based on this theory, all cooling and heating loads can be written in a comprehensive equation. Figure 2-3, shows the heat balance method for an external wall [2]. Additional heating and cooling loads can be added depending on the situation.

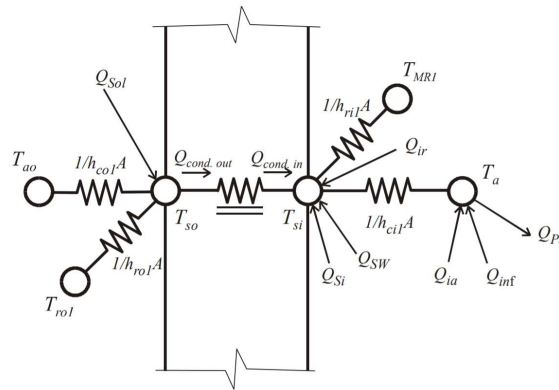


Figure 2-3 ASHRAE Heat Balance Method showing a nodal network for a wall with the outside surface on the left [2]

The ASHRAE method is based on some assumptions. The most important assumption is that the air inside the thermal zone is uniform through the entire zone.

The other assumptions include considering uniform surface temperature, uniform long-wave and short-wave irradiation and one dimensional heat conduction through the walls.

### 2.2.1 Elements in HBM

Based on the heat balance method four distinct processes can be assumed for this method:

- Outdoor-face heat balance
- Indoor-face heat balance
- Wall conduction
- Inside zone air heat balance

Figure 2-4 illustrates the relationships between these processes for a non-transparent wall. The configuration for the transparent surfaces is similar, but the absorbed solar component will be considered in the conduction component instead of outdoor-face heat balance.

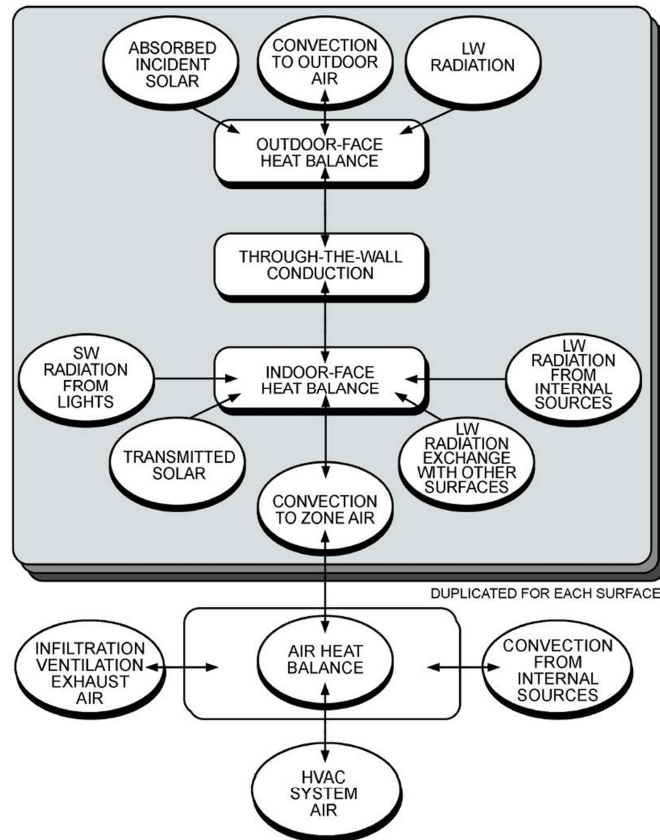


Figure 2-4 Heat balance process in a zone based on ASHRAE HBM [3]

## 2.3 Heat Balance Method (HBM) for vehicles

Heat Balance Method can be used and formulated for a vehicle as well [4]. The comprehensive heat balance ( $\dot{Q}_{Tot}$ ) can be written as equation 2-9. All terms in equation 2-9 will be briefly explained in sections 2.3.1-2.3.8.

$$\dot{Q}_{Tot} = \dot{Q}_{Met} + \dot{Q}_{Dir} + \dot{Q}_{Dif} + \dot{Q}_{Ref} + \dot{Q}_{Amb} + \dot{Q}_{Exh} + \dot{Q}_{Eng} + \dot{Q}_{Ven} + \dot{Q}_{AC} \quad 2-9$$

### 2.3.1 Net overall thermal load ( $\dot{Q}_{Tot}$ )

The net overall heat released to the cabin ( $\dot{Q}_{Tot}$ ) changes the temperature of the cabin. The amount of the temperature change of the inside air at time step of  $\Delta t$  ( $\Delta T_i$ ), can be calculated based on equation 2-10. In equation 2-10, DTM is the overall thermal inertia of the objects

inside the space including seats structures, dashboard, etc.  $m_a$  and  $c_a$  are space air mass and corresponding specific heats of the air, respectively.

$$\Delta T_i = \frac{\dot{Q}_{Tot}}{m_a c_a + DTM} \Delta t \quad 2-10$$

### 2.3.2 Metabolic Load ( $\dot{Q}_{Met}$ )

The human body generates heat and humidity due to metabolic activities. This amounts of heat load ( $\dot{Q}_{Met}$ ), can be estimated based on the relative standards and is associated with parameters such as activity level (i.e. seating, standing, walking, etc.), gender, age, etc. ASHRAE handbook fundamental offers a table for estimation of this term [5].

### 2.3.3 Radiation Loads ( $\dot{Q}_{Dir}$ , $\dot{Q}_{Dif}$ , $\dot{Q}_{Ref}$ )

ASHRAE suggests three categories for radiation loads including direct, diffuse, and reflected radiation loads.

- Direct radiation ( $\dot{Q}_{Dir}$ ) is the part of the solar radiation that directly hits the surface and varies with the angle of incident.
- Diffuse radiation ( $\dot{Q}_{Dif}$ ) is that part of the solar radiation that indirectly strikes the surface and has been scattered by the particles (the water vapor, clouds and dust particles) in the atmosphere.
- The reflected part ( $\dot{Q}_{ref}$ ) is the part of the solar radiation that reflects from the ground or other surrounding surfaces.

### 2.3.4 Ambient load ( $\dot{Q}_{Amb}$ )

Ambient load is the thermal load caused by the temperature gradient between inside air and ambient temperature. Equation 2-11 shows the calculation of ambient load in which  $T_i$  and  $T_s$  are the average cabin temperature and average surface temperature, respectively. In equation 2-11, U or U-Value is the overall heat transfer coefficient consisting of conduction and convection parts and A is the surface area that divides two spaces.

$$\dot{Q}_{Amb} = \sum_{Surfaces} AU(T_s - T_i) \quad 2-11$$

#### 2.3.4.1 U-Value definition

As described in equation 2-12, U-Value is the inverse of the total thermal resistance where R is consisting of inside convection, conduction through the wall and outside convection part. R can be calculated from equation 2-13, in which,  $h_o$  and  $h_i$  are the outside and inside convection coefficients,  $\lambda_j$  is the surface thermal conductivity for layer j, and  $d_j$  is the thickness of the surface element of layer j.

$$U = \frac{1}{R} \quad 2-12$$

$$R = \frac{1}{h_o} + \frac{d_j}{\lambda_j} + \frac{1}{h_i} \quad 2-13$$

### 2.3.5 Ventilation Load ( $\dot{Q}_{ven}$ )

To meet the requirements about the air quality for the passengers and to maintain the CO<sub>2</sub> concentration in an allowable range, a minimum amount of flow of fresh air should be supplied. This flow shall be changed with the number of passengers. There are also air leakages due to the pressure difference between the cabin space and outside space. The corresponding heating and cooling loads for this case should be taken into account using the term “Ventilation load” ( $\dot{Q}_{ven}$ ).

### 2.3.6 Exhaust load ( $\dot{Q}_{Exh}$ )

For vehicles with internal combustion engine (ICG), exhaust gases temperature is rather high. This high temperature gases will lead to a thermal load called exhaust load ( $\dot{Q}_{Exh}$ ).

### 2.3.7 Engine load ( $\dot{Q}_{Eng}$ )

Similar to the exhaust load, when the engine temperature is high, another thermal load related to this source of heat could be supplied to the cabin space. The thermal load is referred to as Engine load ( $\dot{Q}_{Eng}$ ), and mostly is applicable in conventional and hybrid vehicles.

### 2.3.8 AC loads ( $\dot{Q}_{ven}$ )

For keeping the internal temperature in the comfort zone, heating or cooling loads should be added to the space by an air conditioning system. The contribution of air conditioning system is called AC load ( $\dot{Q}_{ven}$ ). Thermal comfort is described in ASHRAE Standard 55.

#### 2.3.8.1 Thermal comfort

Thermal comfort is the requirements related to satisfaction with the thermal environment. It can be measured by two indices PPD and PVM. The acceptable range for each index depends on the standard or specification that will be used. Clothing insulation, air speed, air temperature, radiant temperature, metabolic rate and humidity are the thermal comfort factors. In many cases, it is hard to estimate these factors. Berkeley online tool can be used for the estimations. [6]

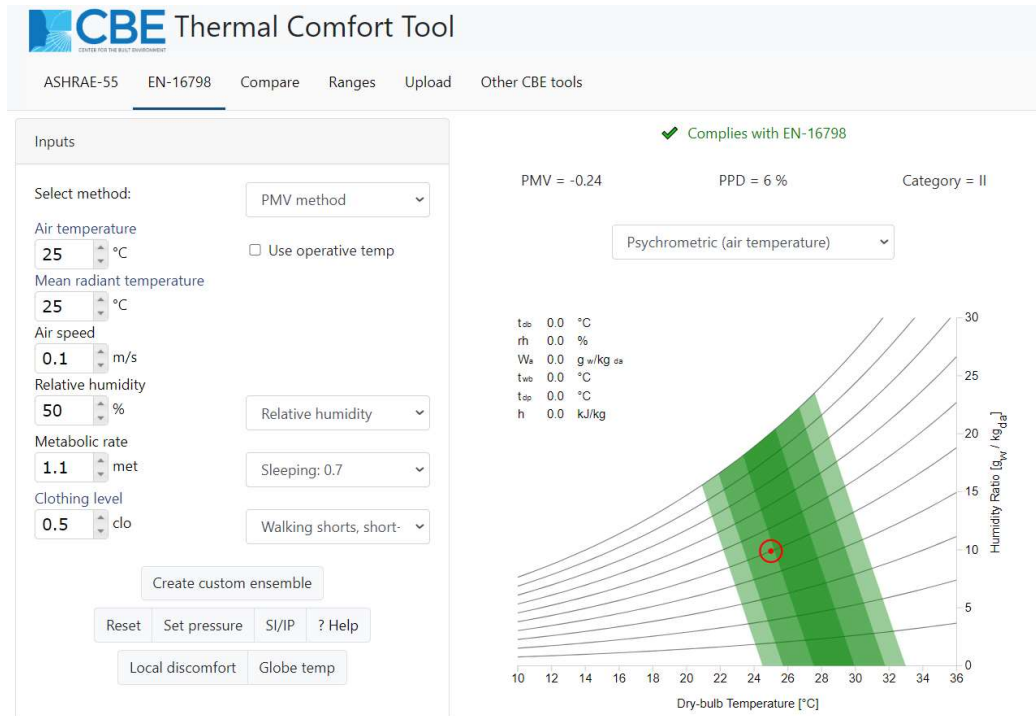


Figure 2-5 CEB tool for thermal comfort prediction [6]

## 2.4 U-value calculation methods

The U-value definition was introduced in section 2.3.4.1. For calculation of U-Value different procedures such as estimated method [7], In Situ Measurement [8], and quantitative methods such as infrared thermography [9] have been suggested. In this work U-Value will be calculated based on the estimated method using two approaches. In the first approach standard suggestions will be used for estimation of surface resistance terms while in the second approach calibrated values will be used for surfaces resistance terms. Calibrated values are the values that will be extracted from simulation software (GT-SUITE) to provide the best match between simulation results and experimental data. Finally, by knowing steady state heat rate and using Eq. 2-11 the U-Value calculated by this approach will also be compared with the two first approaches.

### 2.4.1 U-value calculation estimated method

Standard BS EN ISO 6946:1997, suggests a methodology for U-value calculation in which, the theoretical definition of the U-Value is used.

The first step is defining all material conductivity and thicknesses and creating a network for thermal resistances. Similar to electrical circuit resistance, equivalent thermal resistance can be calculated for parallel and series thermal resistance networks.

### 3 Methodology

In this section the procedure of the work will be described. In first part HVAC system components for an electric bus will be introduced which helps to show the applied thermal loads in an electric bus. In addition, customized heat balance method for an electric bus will be presented. Finally, implementation of the available data for GT-SUITE will be discussed.

#### 3.1 HVAC system Components

For meeting the thermal comfort requirements, heating and cooling load should be added to the cabin. Ventilation and providing fresh air is also another part of laws and regulations related to interior climate requirements. HVAC system works to ensure the interior climate of the bus is in the range of these criteria.

For this electric bus, HVAC system consists of AC system, blowers, convectors and defroster. AC system can be used as a cooling system (cooling load) or heat pump (heat load) depending on the ambient temperature. Blowers, convectors and defroster will be used to heating up the cabin to get the desired temperature and will be considered as heat loads in the model.

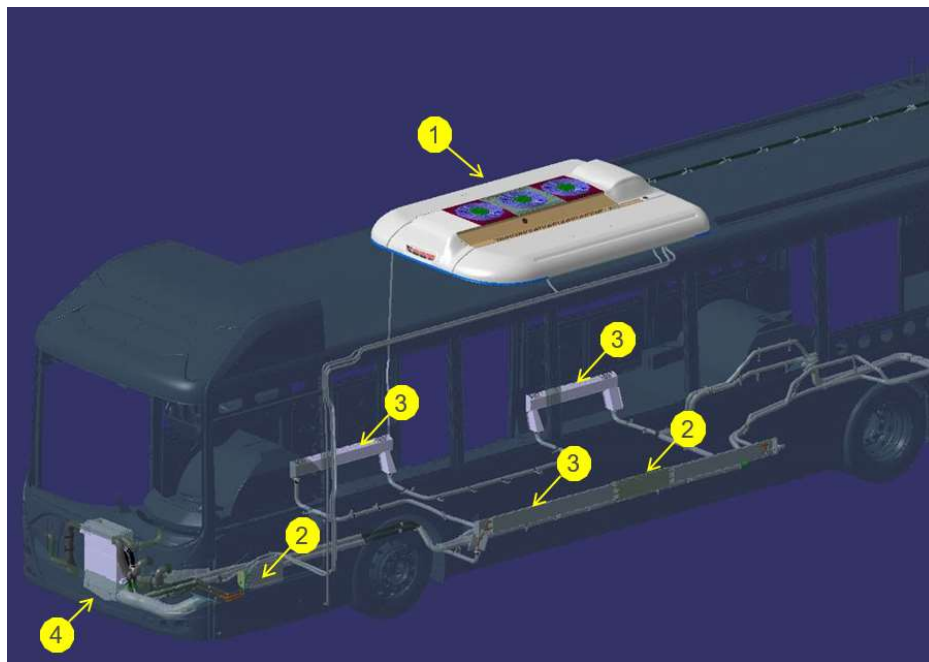


Figure 3-1 HVAC components in the electric bus. 1, 2 and 3 are the AC system, heat blowers, convectors and defroster, respectively.

### 3.2 Heat balance method (HBM) for an electric bus

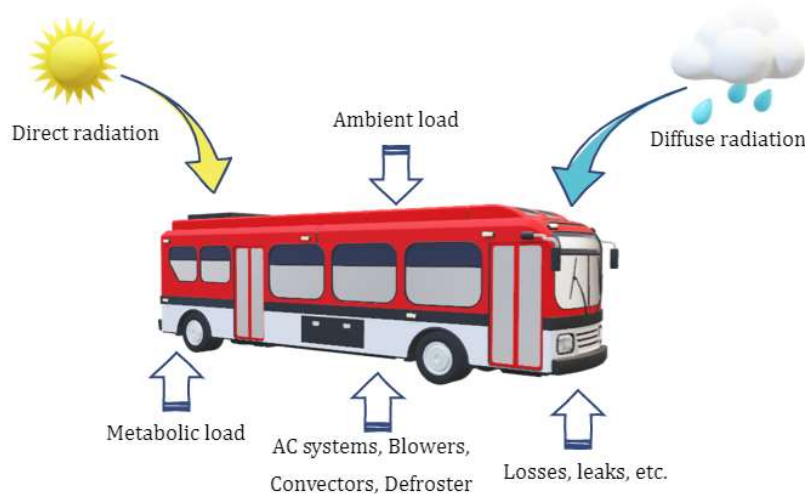


Figure 3-2 Heat balance method for an electric bus

Heat balance method (HBM) will be used for energy declaration of an electric bus. Figure 3-2 shows the applied load for an electric bus. For electric buses, exhaust load would be zero. In addition, engine load can be neglected due to the very low temperature of the electric engine during operation.

Therefore, the heat balance equation for electric buses shall be re-written as equation 3-1.

$$\dot{Q}_{Tot} = \dot{Q}_{Met} + \dot{Q}_{Dir} + \dot{Q}_{Dif} + \dot{Q}_{Ref} + \dot{Q}_{Amb} + \dot{Q}_{Ven} + \dot{Q}_{AC} \quad 3-1$$

This equation shows that the net overall thermal load ( $\dot{Q}_{Tot}$ ) is equal to sum of the all applied loads including metabolic load ( $\dot{Q}_{Met}$ ), solar radiation loads ( $\dot{Q}_{Dir}$ ,  $\dot{Q}_{Dif}$  and  $\dot{Q}_{Ref}$ ) ambient load ( $\dot{Q}_{Amb}$ ), ventilation load ( $\dot{Q}_{Ven}$ ) and air conditioning load ( $\dot{Q}_{AC}$ ).

### 3.3 Simulation using GT-SUITE

In order to achieve a reliable model for different simulation models, as the first step, a model would be calibrated based on the test data. Then, sensitivity analysis will be conducted on this model. As the test have been done in a climate chamber, for calibrated models, solar radiation terms shall be neglected.

#### 3.3.1 Proper model selection in GT-SUITE

GT-SUITE suggests several models for simulation of a cabin. Single-volume zone model and Multi-zone model are two main categories that can be used. For choosing the Multi-zone model the average temperature and heat rate for several zones need to be provided. For this simulation only volume average temperature and heat rate in steady state condition were available from CFD results. Therefore the only choice for modeling this electric bus was single-volume model. In single volume model the average temperature of the cabin will be used for model calibration.

#### 3.3.2 Required input for modelling

Initially, the input data related to the loads shall be defined. The ongoing materials properties and dimensions also shall be measured and entered to GT-SUITE template. The latter data needs some sort of realistic simplifications and assumptions. This part will explain how required data were defined for the first model as a calibrated model.

### 3.3.2.1 General input data

The general data needed for the first model or calibration model, are listed below. These inputs were estimated based on the test conditions and related standards. Table 3-1, shows the applied estimation approach for the calculation of these parameters.

Table 3-1 Estimation approach for setting the parameters – General input

Attribute	Unit	Estimation approach
Ambient Temperature	C	Test data
Vehicle Speed	km/h	Zero for calibration model
Cabin Air Volume	L	Calculated based on the CAD model
External Heat Transfer Coefficient	W/m <sup>2</sup> K	Estimated by GT-SUITE equation
Internal Heat Transfer Coefficient	W/m <sup>2</sup> K	One of the calibration parameters

### 3.3.3 Material definition based on the CAD model

Based on the CAD model which was available in CATIA files, all material geometries including but not limited to surface area and thickness, can be measured. This measurements for a bus cabin can be complicated due to specific geometries and existence of a lot of different materials with different thicknesses and shapes including asymmetric curves and surfaces. For other parts specially wall composition, the estimation is even more complex. Therefore, in many cases assuming equivalent simplified geometries is not avoidable.

### 3.3.4 Calculation of the equivalent U-VALUE for each surface

The equivalent thermal transmittance or U-Value for simple surface parts, will be calculated based on the number of layers, thickness of each layer and thermal conductivity of each layer. For instance, U-Value of surface number “F12” with three layers, shall be calculated as shown in equations 3-2 and 3-3. Where  $d_1$ ,  $d_2$  and  $d_3$  are thicknesses of three different layers.  $\lambda_1$ ,  $\lambda_2$  and  $\lambda_3$  are thermal conductivity of layer 1, layer 2 and layer 3, respectively.  $h_o$  and  $h_i$  are outside and inside convection coefficients which depend on the air velocity and orientation of the surface [4]. These two terms can be estimated based on the standards. In this project outside convection term would be estimated according to BS EN ISO 6946:1997 and inside convection coefficient is one of the calibration parameters in GT-SUITE.

$$U_{F12} = \frac{1}{R_{tot,F12}} \quad 3-2$$

$$R_{tot,F12} = \frac{1}{h_o} + \frac{d_1}{\lambda_1} + \frac{d_2}{\lambda_2} + \frac{d_3}{\lambda_3} + \frac{1}{h_i} \quad 3-3$$

For more complex surfaces, the methodology suggested by BS EN ISO 6946:1997 that was discussed in section 2.4.1 was applied.

### 3.3.5 Average U-Value Calculation of the cabin

The average U-Value of the cabin can be calculated based on the parallel resistance rule and as shown in equation 3-4 where  $U_i$  and  $A_i$  are U-Value and surface area of the surface number “i”, respectively.

$$U_{overall,ave} = \frac{\sum U_i \times A_i}{A_{tot}} \quad 3-4$$

### 3.3.6 Defining average specific heat, density and weight of the elements

The temperature change of the air and cabin mass depends on the mass and specific heat of the materials inside the cabin. Therefore, fraction of the mass and length of the walls including floor, roof and side walls should also be estimated. This estimation was done based on the thickness measurement and calculation of the average density of each element.

### 3.3.7 Defining internal heat gains

The cabin internal heat sources from the miscellaneous equipment and occupants, were estimated based on the test condition. In this case produced heat from lighting and internal equipment such as fans were neglected. For the occupant part the presence of the inspector was considered as an internal source.

### 3.3.8 Defining parameters for thermal comfort prediction

The assumed values for thermal comfort parameters described in section 2.3.8.1 are shown in Table 3-2.

Table 3-2 Estimation approach for setting of parameters –thermal comfort

Attribute	Unit	Estimation approach
Occupant Moisture/Sweat Temperature	C	37
Occupant Moisture/Sweat Input	g/s	0
Occupant Heat Input	W	0
Clothing Insulation (clo)	-	1.1
Activity Level (mets)	-	1
Air Velocity Incident on Body	m/s	0.2

### 3.3.9 Defining initial conditions

For running simulation, initial temperature of the cabin mass, inside air and initial wall temperature should be defined. In the case of calibrated model, the initial temperature for these parts was assumed to be the ambient temperature.

### 3.3.10 Calibration of the model

Since for this work the expected test results were not available, calibration of the model was done based on the available CFD results. In this case, CFD result for “volume average temperature” was used for cabin temperature, and the CFD parameter “input heat rate” was used for cabin heat rate.

Therefore, the model was run based on these CFD results. This model was built based on the data available for stabilized condition. The stabilized condition can be defined as a time interval in which there is a close to zero change in temperature for a constant heat rate of a HVAC system.

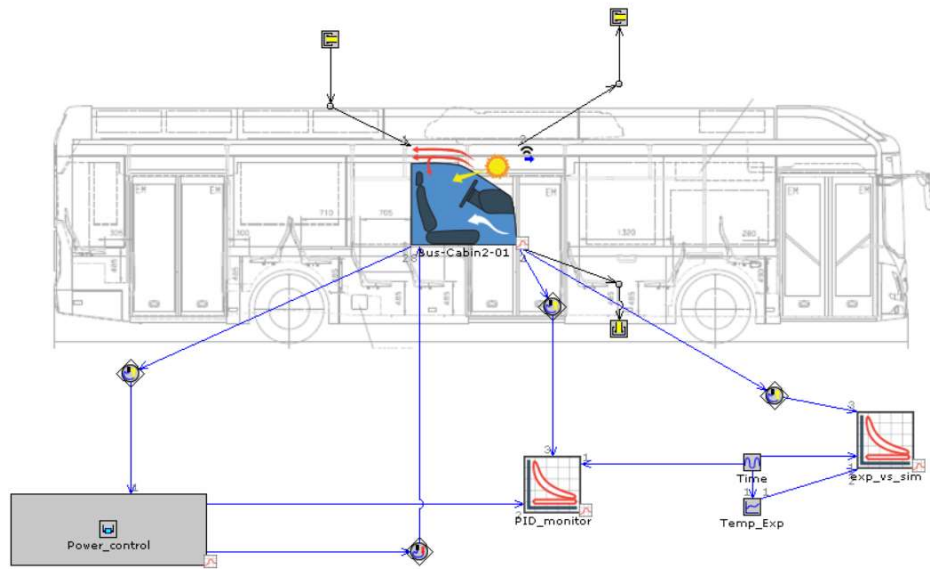


Figure 3-3 Cabin calibration model in GT-SUITE

The CFD simulation had been done based on the available temperatures for six points in a test conducted in a climate chamber. The heat rate for the CFD simulation had been estimated using HVAC equipment's technical data.

As mentioned in section 3, the cabin air will be treated as a lump volume. Therefore, an average temperature for the cabin air was needed to be available. Therefore, the CFD results for steady state case was used to estimate the volume average temperature of the cabin. Figure 3-4 shows the position of these six points.

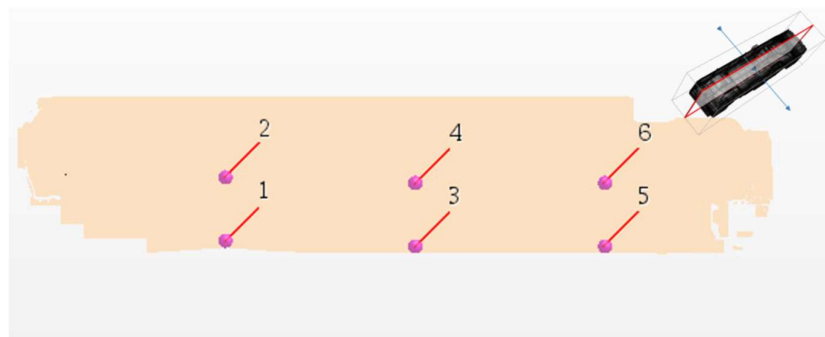


Figure 3-4 Position of six points where the experimental data is measured [10]

For calibration of this model, there were some difficulties due to limitation of obtaining experimental data. The model was calibrated only for one pull-up case and for a steady state condition.

GT-SUITE suggests a transient calibration method for cabin models based on the time-temperature curve. In this model, transient experimental data should be available. By defining calibration parameters and using optimization tool in GT-SUITE the process of calibration will be conducted. GT-SUITE suggests internal heat transfer coefficient and cabin mass as optimization parameters. The optimized parameters will be suggested by GT-SUITE to match the simulation results and experimental data.

The lack of transient experimental data made the process of calibration more complex.

Several ideas for calibration of this model were investigated. The first idea was related to changing the initial conditions. This idea did not work due to the fact that the target temperature

and initial temperature cannot be the same value. For overcoming this problem, initial temperature was set for a value between ambient temperature and target temperature. With this setting and increasing the simulation time, the steady-state condition was achieved and model was calibrated by two parameters internal HTC and cabin mass. The delta T limit for reaching steady-state was set to 0,001 which can be considered as a conservative choice. However, this model's results for high heat rate values would be considered as unrealistic because the cabin reached to the target temperature in a very short time.

Finally, after some try and error attempts, the most reliable results was achieved when the calibration was performed in two steps.

### 3.3.10.1 Calibrate the model in two step

The idea for solving the problem was to calibrate the model in two steps. At first step, calibration of the model was done only with internal heat coefficient and based on the steady-state condition. Secondly, calibrating was performed based on the cabin mass with a transient model.

The advantage of this approach is that generally with only one calibration parameter in each step, the results from GT-SUITE optimizer would be more accurate. But this approach is a bit more time consuming. In addition, it is needed to have a sense of heat rate range and the time before reaching steady state condition. Therefore, here with assuming a reasonable time, the model would be calibrated. This calibration can be improved further by applying an accurate experimental data.

With implying two step approach, the results were reasonable. The steady state temperature in the range of target temperature was achieved and the time that cabin reaches to the target temperature is reasonable. Figure 3-5 shows the results for this approach. Case 1 is calibrated based on the internal HTC with the heat rate related to the stabilized condition. Case 2 is calibrated based on the cabin mass based on the maximum heat rate. It seems that the model gives reasonable results for both cases. However, in case 2 there was another assumption that the maximum power input was applied as a constant value which is not a realistic assumption in many cases. Therefore, another validation should be done for a case with a more realistic initial heat rate.

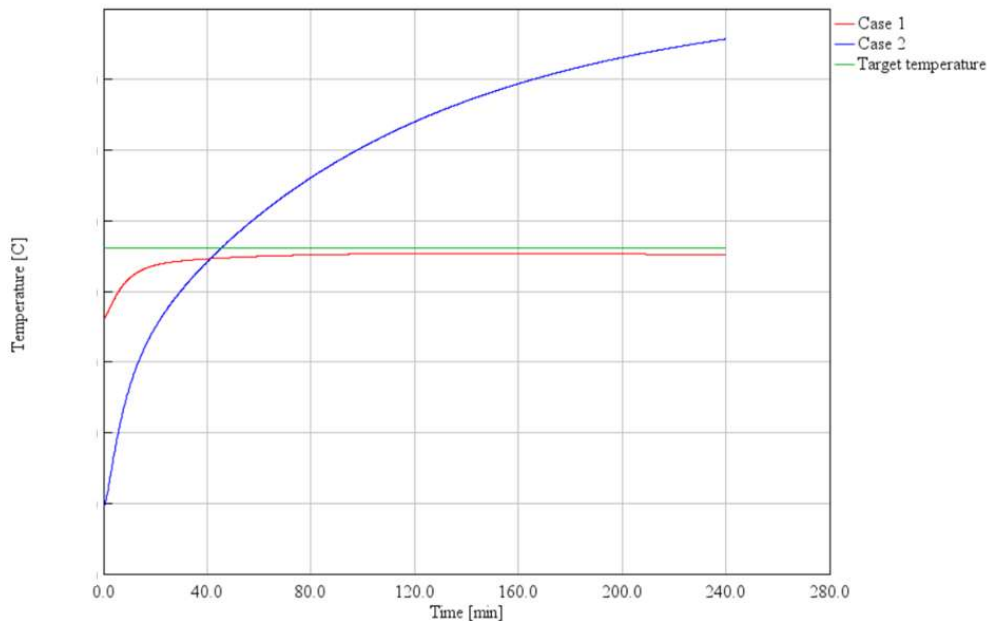


Figure 3-5 Results for two step calibration approach. Case 1 steady state calibration and case 2 transient calibration

### 3.3.10.2 Manually alteration of the initial heat rate

In real tests, depending on the heating systems, it takes a certain time for heaters to work on their maximum capacity. This time depends on the type of heating system. For instance, in a water based heating system, it takes a rather long time to achieve maximum heat rate released to the cabin. This trend would be similar to the condition in which, heat rate is reducing due to the thermal inertia in the system. Therefore, it is needed to estimate a time-heat rate curve before reaching steady-state point. Figure 3-6 shows an example of the heat power rate for a water based heater.

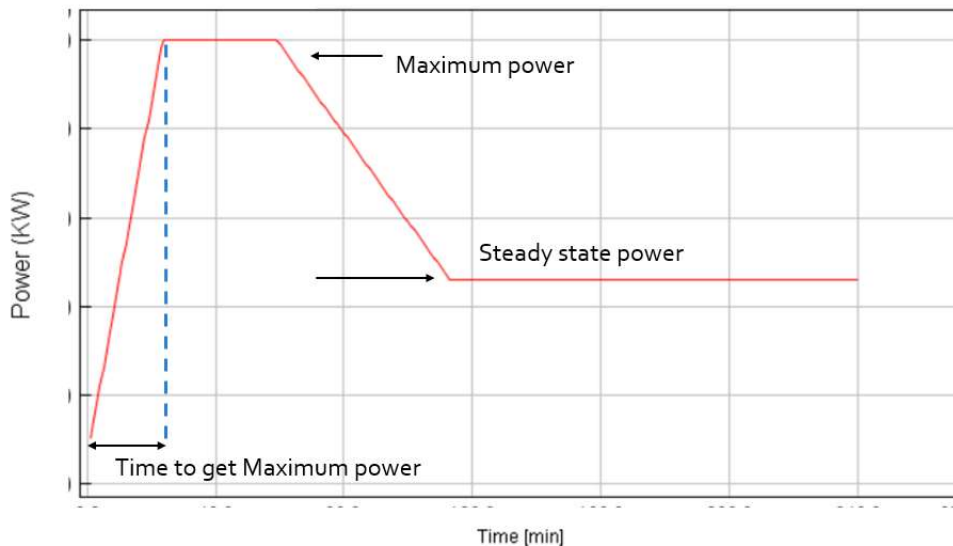


Figure 3-6 An example of the realistic heat rate for the heating system

Simulation results related to the heat rate input can be seen in Figure 3-7.

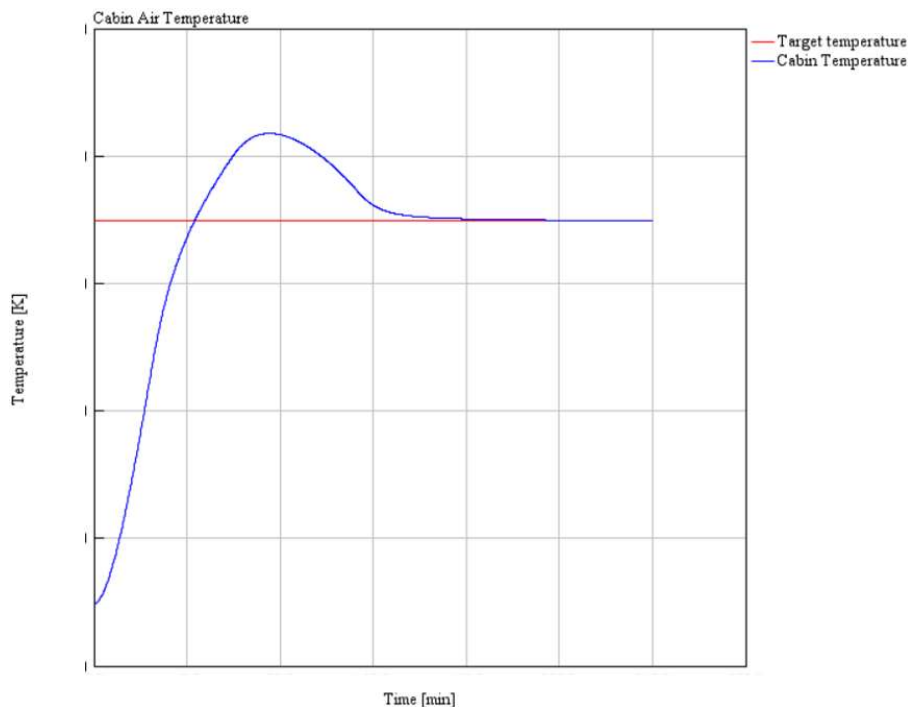


Figure 3-7 Simulation results for a case with a manual heat rate

### 3.3.10.3 Using PID controller for heat rate input

Similar to the manually heat rate control, GT-SUITE suggests PID controller for controlling the power rate based on the cabin temperature. Buses controllers work in a similar way by using sensor's outputs. The results for a case set by PID controller is illustrated in Figure 3-8.

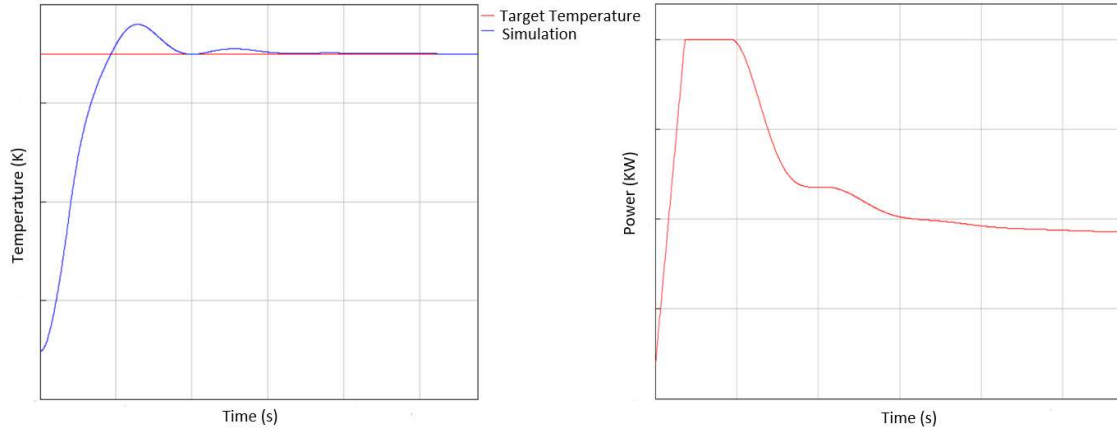


Figure 3-8 Simulation results for a case with PID controller

PID controller settings in GT-SUITE are also illustrated in Table 3-3.

Table 3-3 PID controller setting in GT-SUITE

Attribute	Object Value
Minimum Output	Minimum heater power
Maximum Output	Maximum heater power
Minimum Output Rate	ign
Maximum Output Rate	0.1
Target for the Input Signal	Cabin target temperature
Gains Specification / Calculation	Gains Specified
Proportional Gain	0.01
Integral Gain	0.001
Derivative Gain	0
Derivative Time Constant	def
Other settings	Default

### 3.3.10.4 Optimization method

For model calibration depending on the cases there are several optimization methods suggested in GT-Suite. Settings for design optimizer can be seen in Table 3-4.

Table 3-4 Settings for GT-SUITE Optimizer

Attribute	Object Value
Design optimizer	Integrated Design Optimizer
Optimization Type	Single Objective
Search Algorithm	discrete-grid
Factors	Internal heat transfer coefficient
Response RLT	Cabin air Temperature
Objective	Target
Target Value	Target Temperature

### **3.4 Improving U-Value of the bus's body**

In order to improve the U-Value of the bus three strategies can be conducted: Increasing the material thicknesses, replacing the materials, and adding new materials in the areas that are poorly insulated. In this section some suggestion will be presented for each strategy. In addition, the effect of the change on the total U-Value of the bus will be illustrated. There are some limitations and restrictions when applying each strategy. Changing the total cost of the vehicle, impact on the mechanical properties and impact on the total weight are the most important restrictions for applying these strategies. Basic analysis of applying these criteria can be done by CES software. CES is a material selection software developed by Cambridge University. Design criteria and safety aspects will not be included in this work.

#### **3.4.1 Increasing the material thicknesses**

In some cases, increasing material thickness can be a good idea to decrease the U-Value of the bus. However, there are some limitations for applying this strategy. In this project the effect of increasing the thickness of some insulation materials were investigated.

#### **3.4.2 Adding new materials**

Some parts have the potential for adding new materials. In this case insulation materials are suggested to be added.

#### **3.4.3 Replacing the materials using Ashby bubble plots**

For applying this strategy there are some material properties that should also be considered. Therefore, CES will be used to select between the proposed alternatives.

##### **3.4.3.1 Choosing the plywood for studying alternative materials**

In this work one material was chosen to study the replacement of it by alternative materials. Similar studies can be done for other materials. Calculation of U-Value for different parts of the bus shows that the floor area has the poorest insulation among all parts of the body. For floor area mostly plywood is used. Plywood has a relatively low thermal conductivity and mechanical properties. Having an isotropic stiffness and strength, qualifies the plywood as a good option for applying on the floor. However, rather higher thermal conductivity and higher density of the plywood compared to the other insulation materials, could be a good reason to study the possible alternatives for replacement. Figure 3-9 shows the plywood situation between different materials categories. Some alternative materials with lower density and lower thermal conductivity than plywood exist among foams, elastomers, natural materials, and polymers.

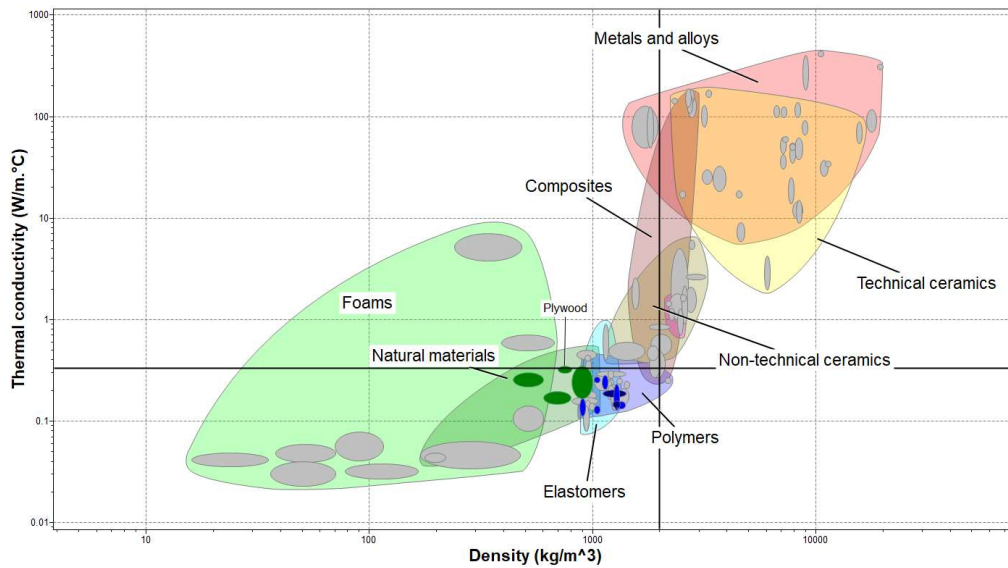


Figure 3-9 Comparison between density and thermal conductivity of different material groups with plywood (CES Results)

This kind of comparison can be done for different materials properties. Figure Figure 3-10 shows thermal conductivity vs young modulus. Young modulus is a mechanical property of materials that represent the stiffness of the material. Young modulus has been chosen among other material properties, since it shows the stiffness of the material which seems to be most important constraint for the component.

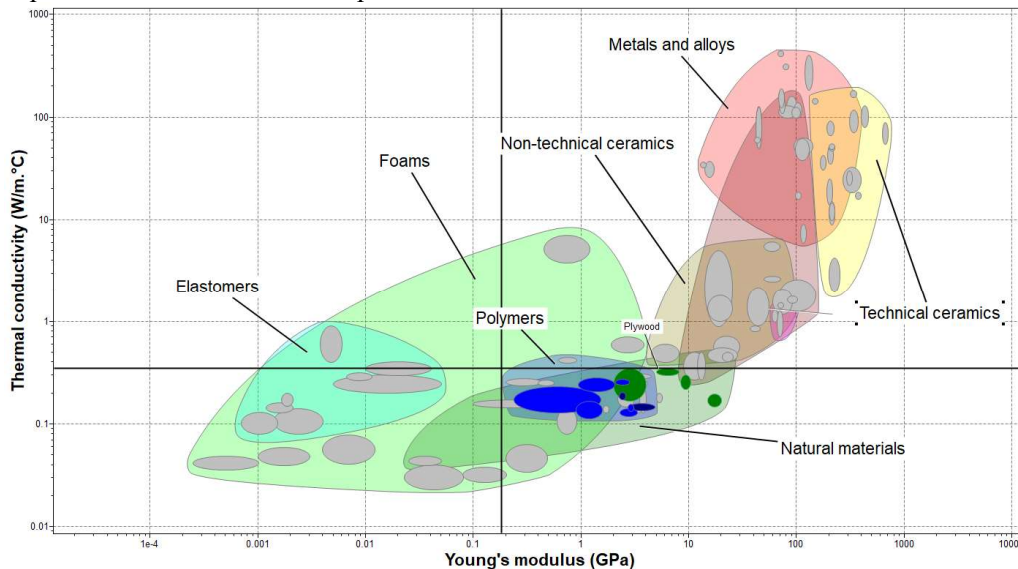


Figure 3-10 Comparison between the conductivity and young modulus of different material groups with plywood.

ASHBY suggests different kind of solutions for a more thorough investigation and finding the proper material index in material selection procedure [12]. One of the suggestions includes determination of the most probable failure condition and select the material having that condition as the constrain of the problem. Considering the working condition of the floor part, the problem can be re-written as shown in Table 3-5. It is worth to mention that the main failure condition has been considered as elastic bending. Depending on the part function or the priorities this constrain can be changed resulting in different material indices.

Table 3-5 Problem translation for material selection of floor part

Problem	Material selection for floor of an electric bus – simplified as a beam with a rectangular cross section.
Constrain	<ul style="list-style-type: none"> <li>• Dimensions of the part are fixed as 15<sub>cm</sub> thickness and area of 26<sub>m</sub><sup>2</sup>.</li> <li>• Lower cost and density are favoured.</li> <li>• Resistance to elastic bending</li> </ul>
Objective	To maximize the U-value or minimize the thermal conductivity
Free variables	Choice of material

The resistance to elastic bending as probable failure condition is illustrated in Figure 3-11.

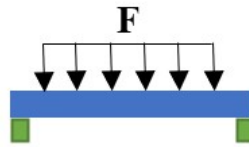


Figure 3-11 Elastic bending condition in floor part

According to Ashby, the deflection of the part can be calculated as described in equation 3-5 in which deflection  $\delta$ , force  $F$ , Young modulus  $E$ , moment  $I$ , failure mode constant  $C_1$  and length  $L$ , have been taken into account. The moment ( $I$ ) for a rectangular cross section can be considered as  $\frac{b h^3}{12}$  in which,  $h$  and  $b$  are the thickness and width of the beam, respectively.

$$\delta = \frac{F \cdot L^3}{C_1 E I} = \frac{12 F \cdot L^3}{C_1 E b h^3} \quad 3-5$$

Therefore, the thickness can be defined as a factor of Young modulus as illustrated in equation 3-6.

$$h = \left( \frac{12 F \cdot L^3}{C_1 E b \delta} \right)^{\frac{1}{3}} \quad 3-6$$

## 4 Results and discussion

In this part the result of several types of models with different parameters, will be discussed. The first model was the calibration model and other models were set depending on the various scenarios.

### 4.1 Calibration model results

Based on the finalized calibration model, it is possible to perform post processing analyses. Figure 4-1 shows the calibrated model's results. In this part results for steady state part would be analysed.

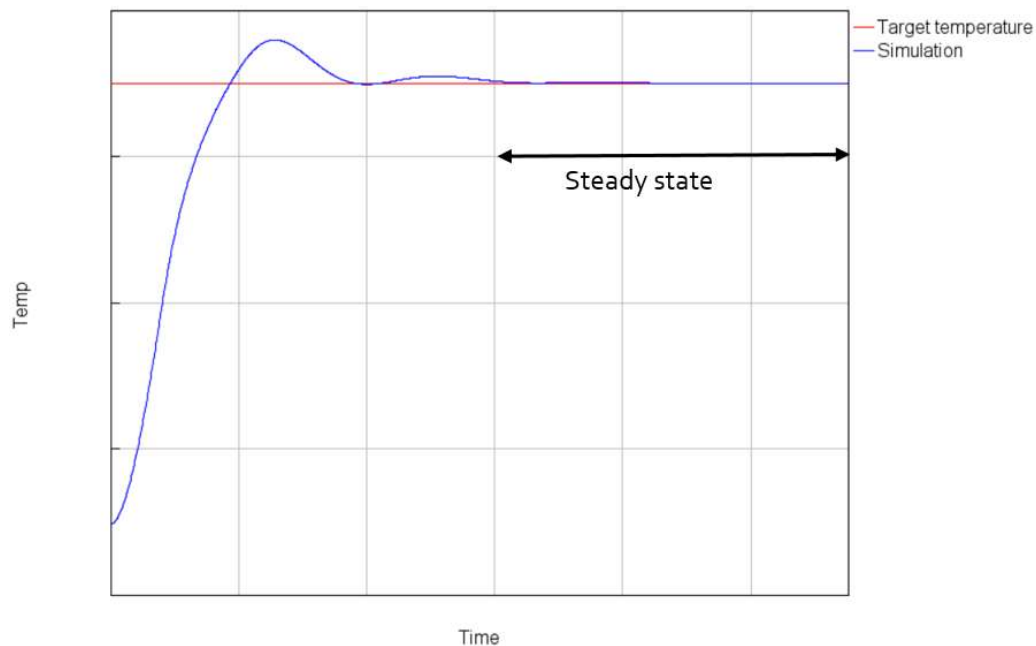


Figure 4-1 Simulation results for the calibrated model

#### 4.1.1 Results categories

Simulation results in GT-SUITE will be shown in different categories. In this part, a brief description about each category is provided. Results can be seen in one point (RLT vs Part) or during the time(Time RLT) in different categories.

##### 4.1.1.1 Main folder

In this folder, results for cabin pressure, internal heat transfer coefficient and external heat transfer coefficient can be found. There are some other items such as vehicle velocity and sun incident angle that was set as a constant parameter for this project. Internal heat transfer coefficient was calculated as a calibration parameter and for external heat transfer coefficient GT-SUITE uses a formulation with the vehicle velocity as a variable. Since in this project vehicle velocity considered to be zero, the external heat transfer coefficient will also be a constant value.

##### Cabin pressure

Cabin pressure is expected to be a constant value in this model since there is no air mass flow input and output. However, the cabin pressure will slightly increase with temperature rise. Figure 4-2 shows the cabin's pressure change trend. This change would lead to pressure difference between cabin air and ambient air and it could cause air leakage if the cabin body is not well sealed.

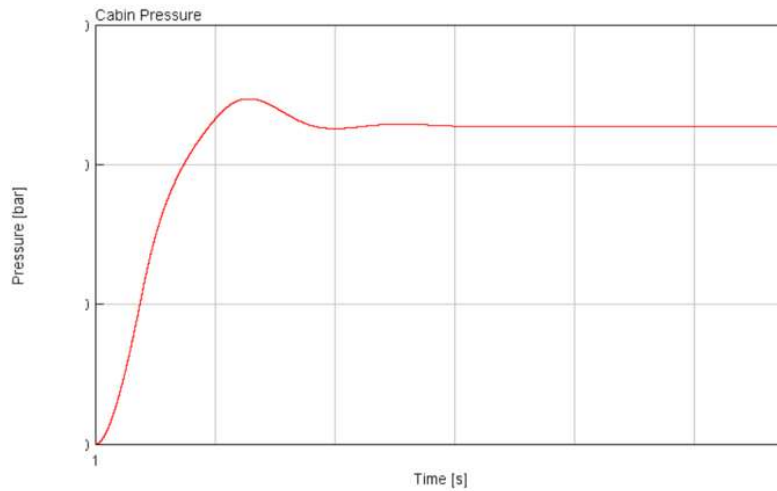


Figure 4-2 Cabin pressure change trend with changing the temperature

#### 4.1.1.2 Temperatures folder

In this folder temperatures for all elements of the cabin bus can be found.

#### Cabin air temperature and “Lumped Mass” temperature

Cabin air temperature is the parameter that should be kept in the desirable range during the simulation. There are two main factors that affects the cabin air temperature: heat rate and cabin mass. “Lumped Mass” temperature is the temperature of the cabin mass. Due to different specific heat constant of the cabin material and air, the trend for increasing and decreasing the temperature of cabin mass and air are different. Figure 4-3 shows the comparison between cabin air and cabin mass temperature change during the simulation time.

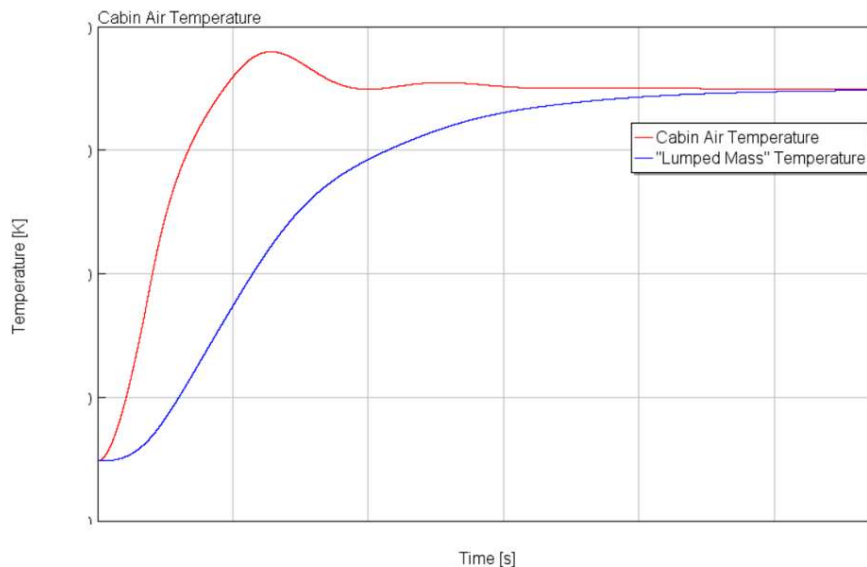


Figure 4-3 Comparison between cabin air temperature and cabin mass temperature

As it can be seen in Figure 4-3, lumped mass temperature is less affected by changing the heat rate while the cabin air temperature has some oscillations.

Due to the higher heat capacity, cabin mass temperature increases and decreases less dramatically. This behaviour is due to the effect of thermal inertial presented in Eq. 2-10.

Thermal inertia is an important phenomenon that should be considered in design of HVAC systems.

### Element temperatures

In this folder, temperatures for other elements such as walls and roof can be found. In addition, it is possible to check the temperature for inside, outside and center of elements. This folder, provides a good sense about changing the temperature inside each element. Figure 4-4 shows the temperature trend for different parts of the roof element.

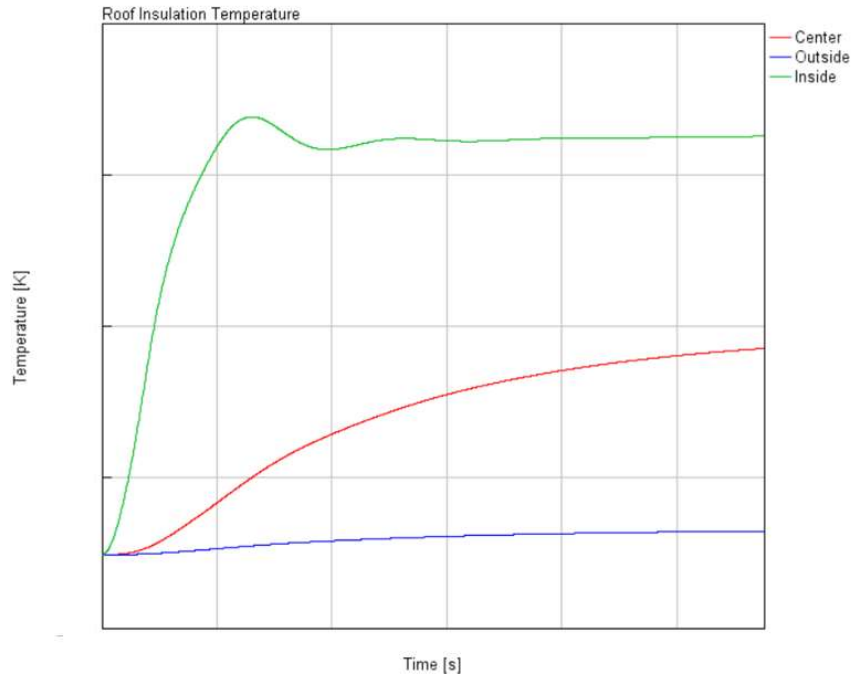


Figure 4-4 Roof insulation temperature trend during the simulation in different parts, inside, outside and center

### 4.1.1.3 Internal heat rates and external heat rates folders

Internal and external heat rates for all surfaces are another parts of the results which can be subjected to analyses.

The summation of the internal heat rates is equal to the heat rate released to the cabin. Figure 4-5 shows the results for internal heat rates in different elements of the bus.

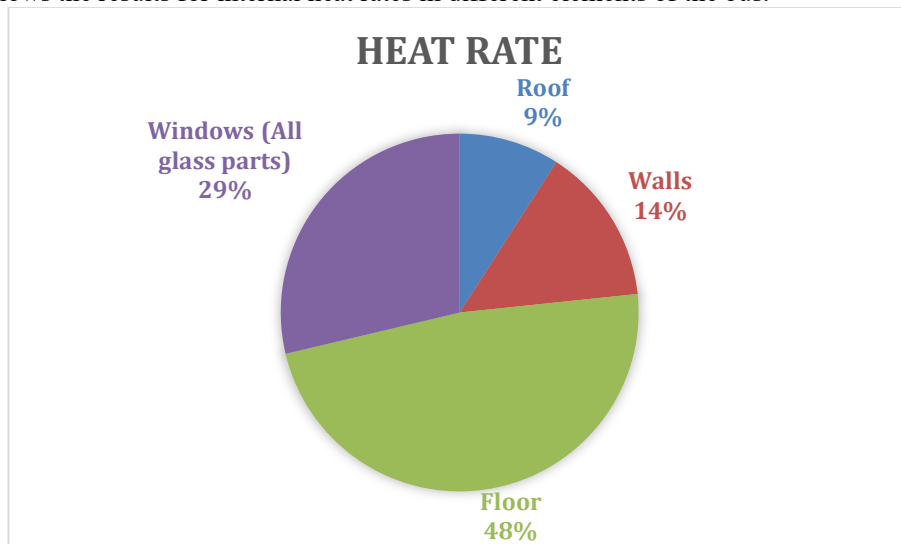


Figure 4-5 Calculation of U-Value for bus's part based on the heat rate results from GT-SUITE

This data provides the heat rates for different elements of the body. The results shows that 50% of the heat transfer is occurred in the floor area. It means that this area is poorly insulated and half of the heat losses occurs in this area. But this conclusion is not reliable. Figure 4-6 and Figure 4-7 illustrate the CFD results for a similar case on this bus [10]. Based on Figure 4-6 and Figure 4-7, the temperature distribution could be in a range up to 40 °C inside the cabin meaning that equation 2-11 cannot be applied for all elements. However, since  $T_i$  in equation 2-11 is higher than the average air temperature in some areas and lower in some other areas such as floor, for similar cases, overall heat transfer coefficient can be roughly estimated. An attempt can be made to solve this issue by defining a multi-zone model. In section 4.3.2 the multi-zone model will be explained in more details. However, for energy consumption calculation it is possible to adjust different temperature gradients for different parts.

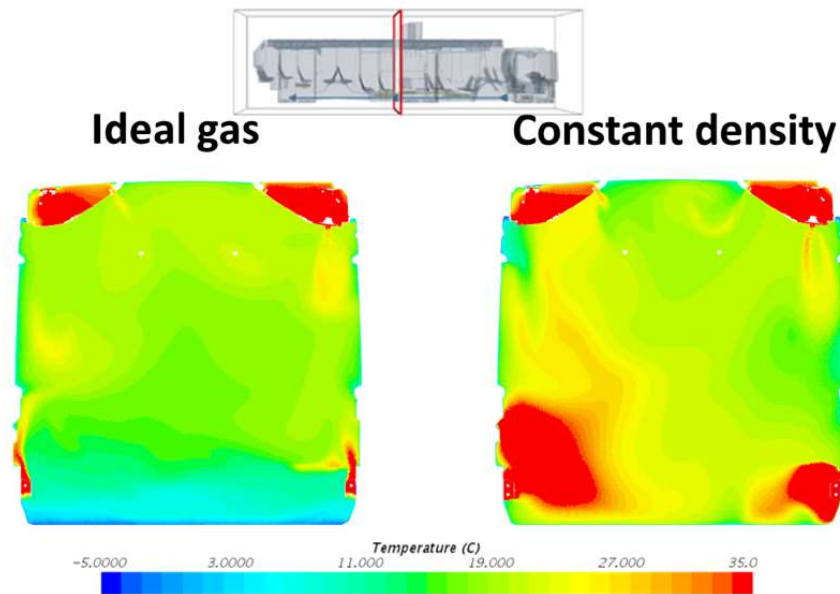


Figure 4-6- A CFD results shows temperature distribution for a similar case

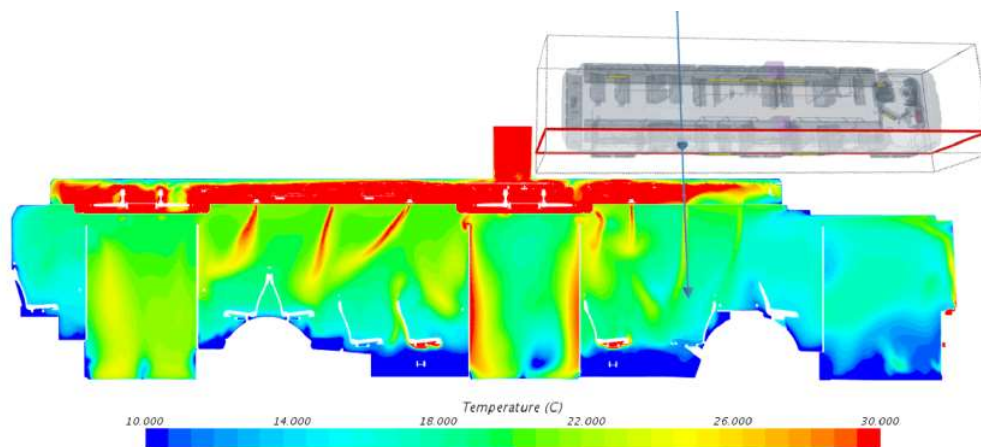


Figure 4-7 CFD results that shows temperature distribution in a steady state case

#### 4.1.1.4 Thermal comfort prediction

Based on the parameters for thermal comfort prediction explained in section 3.3.8, GT-SUITE predicts thermal comfort according to the PPD and PMV factors. These factors are clothing insulation, air speed, air temperature, radiant temperature, metabolic rate and humidity.

However, for achieving more accurate results, thermal comfort parameters, special air speed and humidity should be defined based on the experimental data. In this work, only the trend of thermal comfort prediction factors would be studied. Figure 4-8 shows the PPD factor during the simulation time. The graph shows that for getting a better PPD factor, higher temperature is required. But as previously mentioned, without having information about other parameters and a temperature resolution that shows the temperature on the different parts of the body, this result cannot be considered as a reliable evaluation factor for thermal comfort prediction.

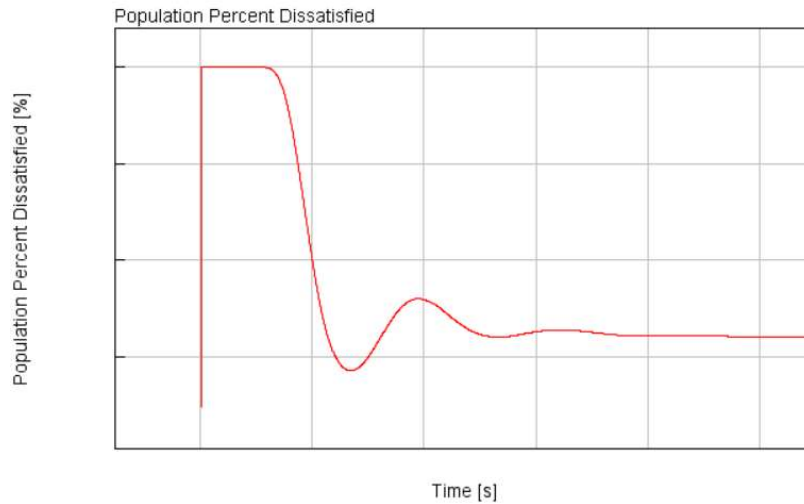


Figure 4-8 PPD result during the simulation time

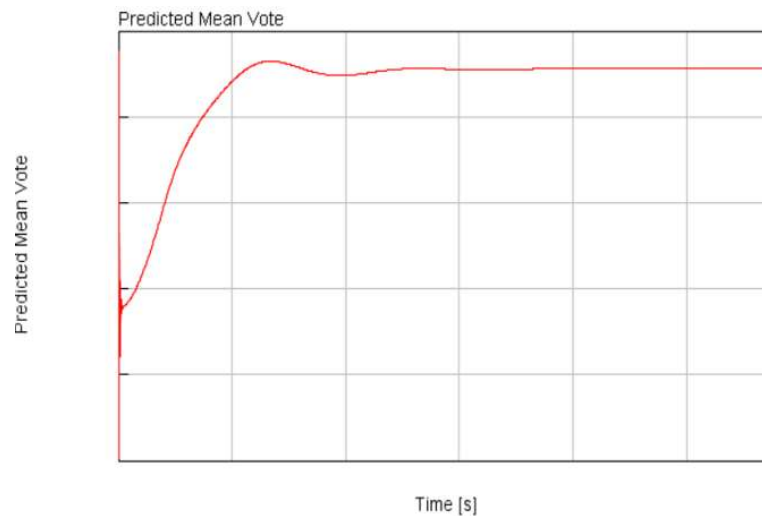


Figure 4-9 PVM result during the simulation time

#### 4.1.1.5 Fog prediction

Fog prediction in GT-POST will be indicated with two indices: 1 for fog formation and 0 for no fog. Results show no fog for all windows.

## 4.2 Calculation of the U-Value with different approaches

In this part the calculation results for U-Value of the bus with three different approaches will be presented and compared.

### 4.2.1 U-Value calculation based on the estimated method by defining the HTC based on the standards

As discussed in section 2.4 Standard BS EN ISO 6946:1997 suggests corresponding values for internal and external heat transfer coefficients. These values are suggested for buildings. However, using them for a stationary vehicle could be accepted.

### 4.2.2 U-Value calculation based on the estimated method using HTCs from GT-SUITE results

In this approach estimated method was used. GT-SUITE results for internal and external heat transfer coefficient were used for defining parameters  $h_o$  and  $h_i$  in equation 2-13.

### 4.2.3 U-Value calculation based on the heat rates from GT-SUITE results

GT-SUITE results for heat rates that are presented in section 4.1.1.3 can be used for calculation of the U-Value for each part of the bus. By defining the surface area of each parts and using equation 2-11 the corresponding U-Value for all elements can be calculated. By using equation. 3-4, the overall U-Value can also be calculated.

As it was expected the result from this approach is quite close to the previous approach.

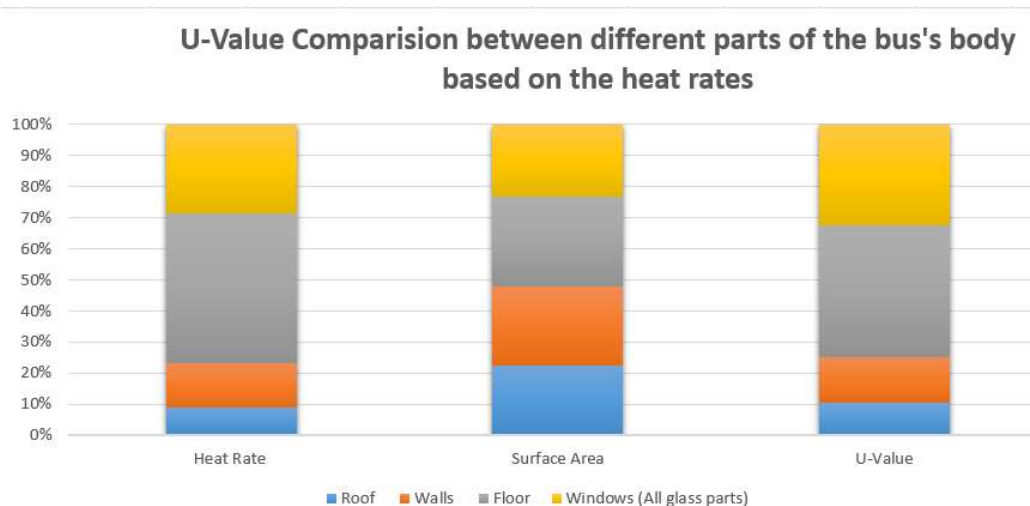


Figure 4-10 U-Value calculation based on the heat rates for different parts of the bus

### 4.2.4 Comparison between U-Values from different approaches

Figure 4-11 shows the comparison between U-Value calculations with different approaches. Results for first approach was around 30% higher than the two other approaches. It means that internal and external heat transfer coefficients suggested by GT-SUITE are lower than the ones can be found in standards.

### U-Value calculation results using three different approaches

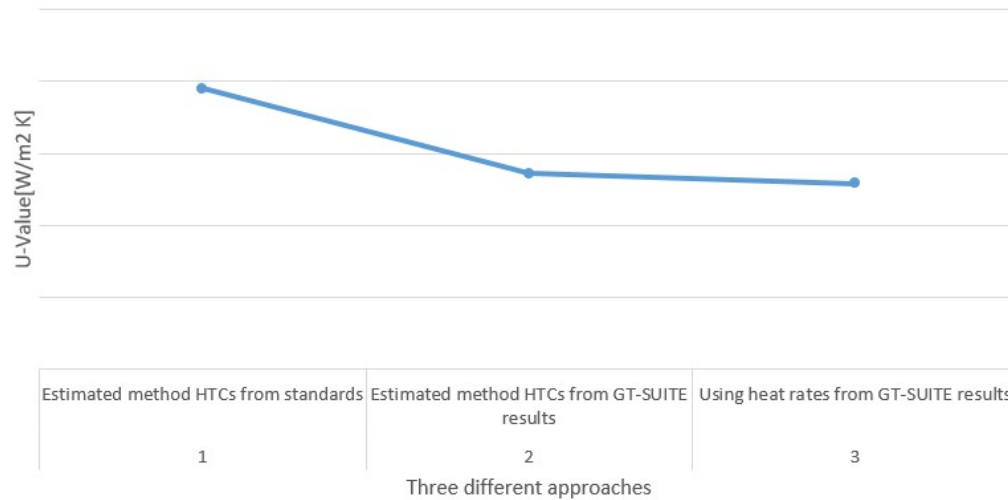


Figure 4-11 Comparison between U-Value calculation results from three different approaches

The results for the first approach can be assumed as the less accurate procedure. This conclusion is due to the fact that there were some sort of simplifications and assumptions during the process of the calculation of the U-Value without any experimental data to validate these assumptions.

## 4.3 Suggestions for improving the model’s accuracy

In this part some suggestions for improving the model’s accuracy for future works will be presented.

### 4.3.1 Calibration the model for a transient model

The cabin model is now enough reliable to study other different scenarios and perform a sensitivity analyses. The model has been calibrated based on the steady state condition. However, with transient experimental data, it is expected to have a more accurate model. It is due to the fact that in transient model, the model provides accurate results for all time resolutions at least for several points.

### 4.3.2 Using multi-zone model

For this work, a single-volume model was used. It means a homogeneous temperature was assumed. This assumption for most HVAC systems gives acceptable results. However, in reality different areas have different temperatures. In multi-zone cabin model the volume of the cabin will be divided to several lump volumes and the average temperature and heat rate can be set for each zone individually. This model will give surely more accurate results but it requires more experimental data.

### 4.3.3 Adding HVAC equipment to the model

This model use a net heat rate input. In most cases, this heat input will be considered as a constant value. However, AC systems and heat pumps give different outputs in different weather conditions. It is possible to combine the refrigerant cycle to the model. Adding the refrigerant cycle, promotes the model since the possibility of studying the effect of replacing the refrigerants can be investigated.

Figure 4-12 shows the cabin model integration with HVAC system.

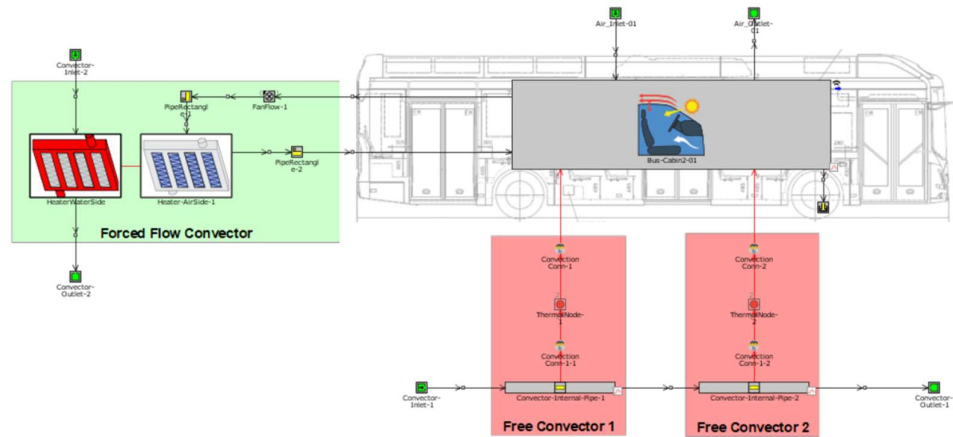


Figure 4-12 Cabin model integration with HVAC system (GT-SUITE tutorials)

#### 4.3.4 Applying door opening schedules

For studying the real driving cycles especially when it comes to the city buses, applying the door opening schedule is necessary. The GT-SUITE customized cabin model has this possibility to set different door opening schedules. However, some additional experimental data for estimation of the mass flow rate entering the cabin during the time that doors open to pick up the passengers, would be required.

Similar to the cases with closed doors, calibration of the model can be done based on the transient experimental data.

### 4.4 Comparison between estimated U-Values and infrared photos

With defining the internal heat coefficient and external heat coefficient, the U-Value for different parts can be estimated. The higher U-value corresponds to the areas with poorer insulation. During the test when the cabin temperature reaches the target temperature, there are different heat rates in different parts of the body causing different temperatures on each parts of the body. Available infra-red photographs could be a good tool to compare the temperature of the different body parts.

The results from the estimated method were compared with the available infra-red photos. This comparison confirms that the parts with highest calculated U-Value are the ones that interpreted to have poor insulation based on the infra-red photos.

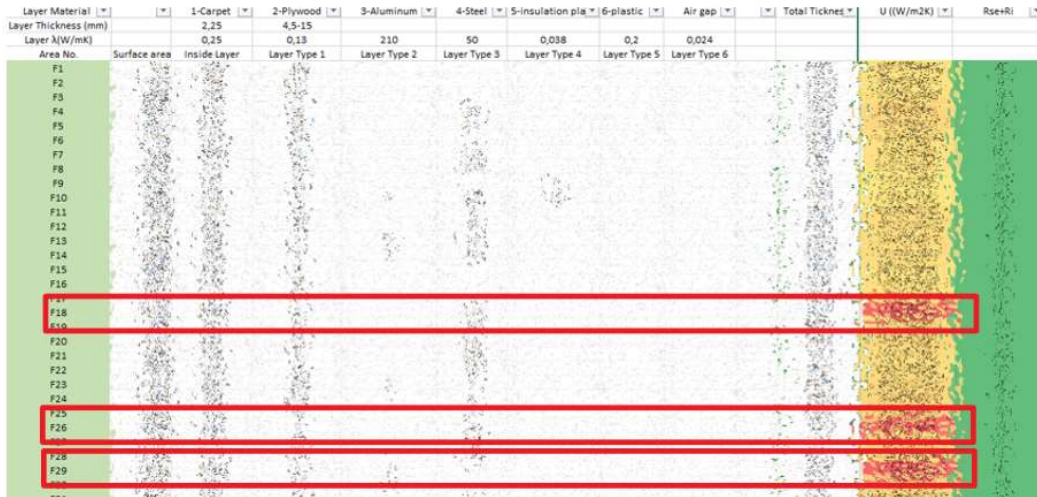


Figure 4-13 Areas with higher U-Values based on the calculation

## 4.5 Suggestions for improving the U-Value of the bus's body

According to the explanations in the section 3.4, some suggestions can be presented for improving the U-Value of the bus. As previously mentioned in the methodology section, three strategies will be investigated: increasing the material thicknesses, replacing the materials, and adding new materials in the areas that are poorly insulated.

### 4.5.1 Increasing the material thicknesses

Increasing the Roof insulation thickness was investigated for this part. Roof's insulation thickness was 20% increased. Results for increasing the roof's insulation thickness can be seen in the Table 4-1.

Table 4-1 Results for applying increasing material's thickness strategy

Improving Method	Change in thickness of roof's insulation (%)	change in roof's U-Value (%)	Change in total U-Value (%)	Change in energy usage (%)
Increasing thickness	20	8,7	0,93	0,93

The effect of this change on the U-Value is not significant. It was expected since the U-Value of the roof was quite low before this improvement.

### 4.5.2 Adding new materials

Considering design limitations adding 3mm Polyethylene (PE) foam to Pillar parts was investigated. The impact of this change can be seen in Table 4-2.

Table 4-2 Results for applying adding insulation materials strategy

Improving Method	Thickness of added PE foam(mm)	Change in total U-Value (%)	Change in energy usage (%)
Adding insulation materials	3	2,9	2,9

### 4.5.3 Replacement of the materials using Ashby bubble plots

According to the methodology suggested in section 3.4.3.1 for replacing plywood with a better alternative from the thermal conductivity point of view, the result can be obtained in two stages. In both stages, the Young modulus criterion was investigated and in the second stage based on the CES database cost data also can be taken into account.

#### 4.5.3.1 Stage 1: Young modulus criterion

Having the relationship between U-value and thickness as described in equation 2-12 and considering the thickness as described in equation 3-6, the U value now can be re-written as shown in equation 4-1. In equation 4-1, the first term is the fixed terms as defined by component function while the second term ( $\lambda E^{\frac{1}{3}}$ ) is about material properties and it is called the first material index  $M_1$ . Since the objective is to minimize the U-value, the same shall be applied on the material index.

$$U = \left(\frac{C_1 b \delta}{12 F \cdot L^3}\right)^{\frac{1}{3}} \times \lambda E^{\frac{1}{3}} \quad 4-1$$

Due to logarithmic scale in Ashby bubble plots, this material index will be presented by line with a slope of (-3) when plotting Young modulus versus thermal conductivity in CES software (material selection software developed by Cambridge University) in Figure 4-14.

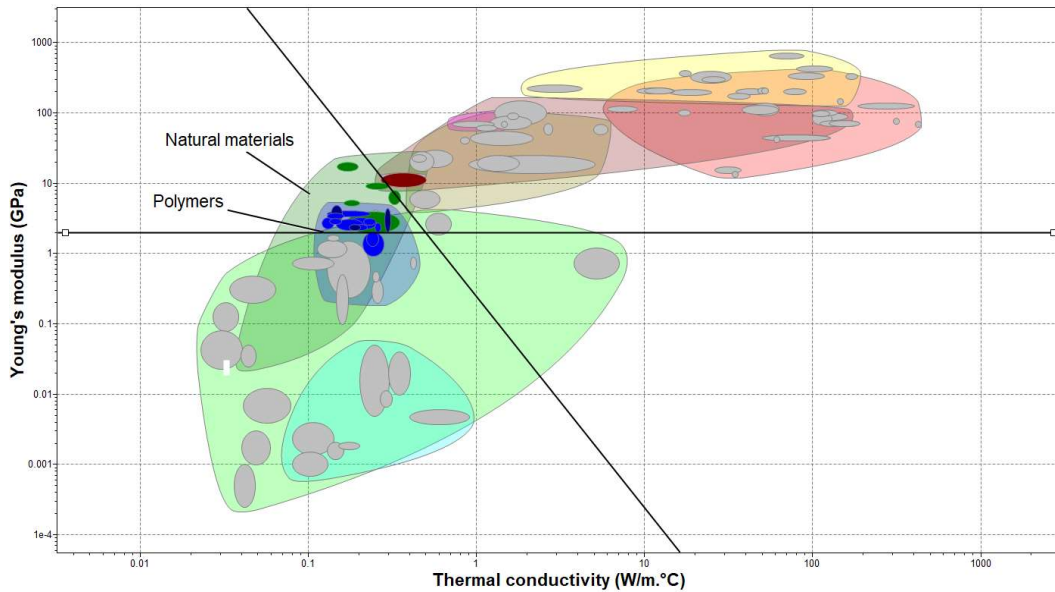


Figure 4-14 Ashby plot for Young modulus vs Thermal conductivity

All the materials on the left side of this line in Figure 4-14 would qualify for lowering the U-value. By determination of minimum acceptable stiffness of the material as having Young modulus above 2 GPa, and setting the material index line to cross the material is already used in this component (plywood) the alternative choices will be presented by software as shown in figure Figure 4-14 and summarized in Table 4-3. The alternatives mainly belong in polymer and natural material groups.

Table 4-3 Alternative materials suggested by CES after first stage

Alternative materials for floor part of bus after applying first material index
Acrylonitrile butadiene styrene (ABS)
Bamboo
Epoxies (EP)
Hardwood: oak, across grain
Paper and cardboard
Phenolics (PH)
Plywood
Polyamides (Nylons, PA)
Polycarbonate (PC)
Polyester (UP)
Polyetheretherketone (PEEK)
Polyethylene terephthalate (PET)
Polyhydroxyalkanoates (PHA, PHB)
Poly lactide (PLA)
Polymethyl methacrylate (Acrylic, PMMA)
Polyoxymethylene (Acetal, POM)
Polystyrene (PS)
Polyurethane (tpPUR)
Polyvinylchloride (tpPVC)
Sheet molding compound, SMC, polyester matrix
Softwood: pine, along grain

#### 4.5.3.2 Stage 2: Price criterion

The price can be considered as an objective to be minimized for the second material index. As illustrated in equation 4-2, the cost of component (P) can be calculated based on its surface area A, the thickness h, density  $\rho$  and cost per kilogram C.

$$P = A \cdot h \cdot \rho \cdot C \quad 4-2$$

By replacing the thickness in equation 4-2 from the thickness obtained from equation 3-6, the equation shall be re-written as shown in equation 4-3 in which, the first terms are constants defined by the problem and second term ( $\frac{\rho \cdot C}{E^3}$ ), only includes the material properties and shall be called second material index  $M_2$ .

$$P = A \left( \frac{12 F \cdot L^3}{C_1 b \delta} \right)^{\frac{1}{3}} \times \frac{\rho \cdot C}{E^3} \quad 4-3$$

This material index is represented by a line with the slope of 3 as indicated in Figure 4-15, in which Young modulus is plotted against cost per kilogram C times density.

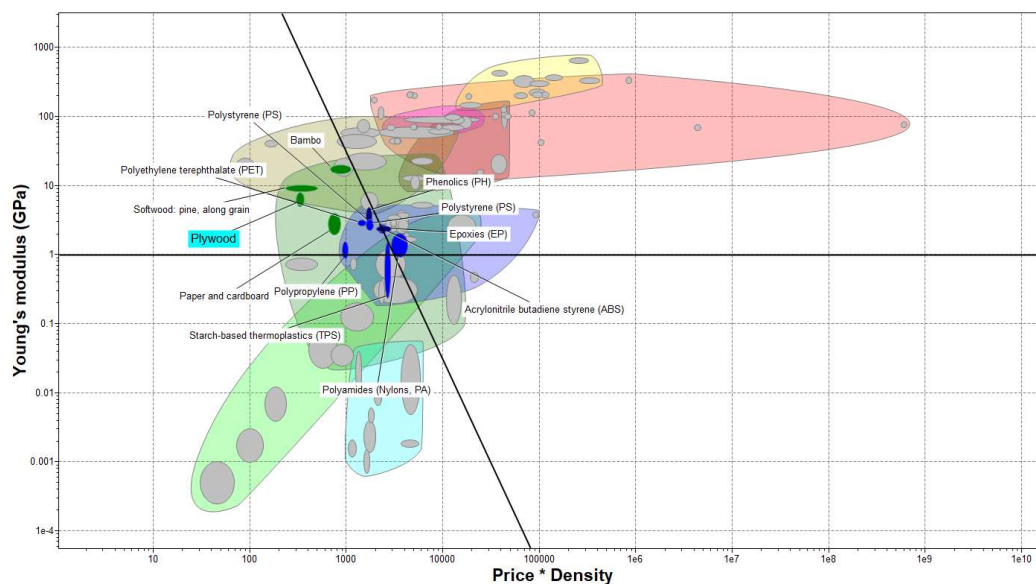


Figure 4-15 Ashby bubble plot for Young modulus vs density times cost per kilogram

Alternative materials listed in Table 4-3, will be limited to materials listed in Table 4-4 when applying the second material index in addition to the first material index.

Table 4-4 Alternative materials suggested by CES software after second stage

	Density [kg/m <sup>3</sup> ]	Price [GBP/kg]	Young modulus [GPa]	Thermal conductivity [W/m.°C]
Polystyrene (PS)	1,04E+03	1.55-1.8	2.28-3.28	0.12-0.14
Poly lactide (PLA)	1.24e3-1.27e3	2.14-2.82	3.31-3.58	0.13-0.16
Polyethylene terephthalate (PET)	1.29e3-1.39e3	1-1.17	2.79-3.01	0.134-0.156
Phenolics (PH)	1.24e3-1.32e3	1.26-1.42	2.77-4.82	0.136-0.158
Polyvinylchloride (tpPVC)	1.29e3-1.45e3	1.94-1.97	2.19-3.11	0.147-0.209
Bamboo	602-797	1.02-1.52	15.1-19.9	0.148-0.195
Paper and cardboard	808-996	0.749-0.922	2.00-4.00	0.17-0.347
Epoxies (EP)	1.11e3-1.4e3	1.72-2.2	2.27-2.55	0.174-0.203
Softwood: pine, along grain	440-600	0.471-0.941	8.4-10.3	0.22-0.3
Acrylonitrile butadiene styrene (ABS)	1.03e3-1.06e3	2.05-2.47	2.08-2.75	0.253-0.263
<b>Plywood</b>	699-801	0.419-0.462	5.02-7.97	0.3-0.35

#### 4.5.4 Studying the effect of replacing plywood with one of the alternatives

Based on the CES results, one of the acceptable alternatives can be chosen to check the impact of this replacement on the U-Value of the floor and total U-Value.

Table 4-4 shows the alternative materials for plywood sorted based on the thermal conductivity. Polymers have much better insulation properties but with lower Young modules. It means with considering a Young module in range of plywood, the only options are once again among natural materials, bamboo and softwood. Since bamboo is rather expensive, the only alternative may be considered as softwood with slightly better thermal conductivity and the price in the range of the plywood. The other fact is that the values that suppliers offer are much lower than the ones can be found in references and CES in this case. Despite these facts the study can be done with this assumption that the plywood thermal conductivity can be improved either with replacing by softwood or with a better plywood from the thermal conductivity point of view. In addition, the possibility of applying structural adjustments (e.g. sandwich panels) to the component resulting in better mechanical response, have been avoided in this project. If those adjustment are possible from technical point of view, the possibility of replacing polymers with them can be investigated.

Table 4-5 shows the effect of replacing plywood with a sandwich panel with 50% lower thermal conductivity.

Table 4-5 Results for applying material replacement strategy

Improving Method	Change in material conductivity (%)	change in floor's U-Value (%)	Change in total U-Value (%)	Change in energy usage (%)
Material replacement	50	23,2	14,9	14,9

#### 4.5.5 Replacement of the side windows

Another sensitivity analysis was conducted for a case that side windows were replaced with windows with 35% lower U-Value. Table 4-6 shows the results regarding this change.

*Table 4-6 Results for side windows replacement*

Improving Method	Change in U-value (%)	Change in total U-Value (%)	Change in energy usage (%)
Windows replacement	35	3,11	3,11

## 5 Conclusions

This master thesis work presented the methodology for calculation of the U-Value for the Volvo electric bus. The energy model for the Heating Ventilation and Air Conditioning (HVAC) system was developed and calibrated for the purpose of the U-value calculation. The simulations were performed using the GT-SUITE, a system-level simulation software developed by Gamma Technologies.

By using calibrated parameters from the simulations the accuracy of the U-Value calculation based on the estimated method was increased. Calibrated parameters compensate the uncertainties in the calculation of the conductive parts in the U-Value calculation. Therefore, the heat transfer coefficient provided by this model will be valid only for the case that calibration is done for that based on the test data. This approach is promising since assuming simplified geometries for bus's body is unavoidable especially in cases with air gaps where it is impossible to calculate the equivalent U-Value without uncertainties.

It should also be noted that in this work the steady-state calibration was done and analyses is reliable for steady-state condition. It means that for a comprehensive study on this case, transient test data should be collected and the model shall be calibrated based on these transient experimental data as well.

The next conclusion is related to the selection of the appropriate model. There are available models with different levels of accuracy and details. For system focus analyses, single-volume models give desirable results. The simulation is faster for these models making them suitable for simulating longer time durations. Less experimental data required is another reason for choosing this model. For thermal comfort studies multi-zone models give more accurate results. In multi-zone models calibration can be done for each zone and in contrast with single-volume models, it is possible to calibrate heat transfer coefficients for different surfaces.

For other analyses, such as studying the effect of HVAC equipment performances in different ambient temperatures, studying the impact of changing the refrigerant in AC system, analyzing the heaters performance, etc., GT-SUITE suggests appropriate models as well.

U-Value improvement approaches were also analyzed in this work. However, there are several technical and economic constraints that should be taken into account in the redesign procedures. The energy saving estimations should also be done based on the more accurate models.

The simulation of the real-world driving cycles can be done using the calibrated models. Applying door opening schedules for these simulations is also necessary. The calibrated model in this project has the possibility to add the door opening schedules.

It should also be mentioned that the model was calibrated only for one pull-up case. Due to the fact that thermal conductivity varies with temperature for some materials, it is recommended to calibrate the model for a pull-down case, as well as for simulating in warm weather conditions. Finally, it is possible to run the simulation for real cycles by entering the required data such as speed profiles, weather data, solar radiation factors, etc. into GT-SUITE. Gamma technology also suggests a separate platform for this purpose. Simulation of real drive cycles is important in many aspects. It provides replacement and complement for expensive physical tests. In addition, it gives a good overview for end users to estimate the amount of energy consumptions based on the region and conditions that they use the vehicle.

## 6 References

- [1] J. H. L. I. & J. H. L. V, A Heat Transfer Textbook, Massachusetts: Phlogiston Press, 2019, pp. 52-53.
- [2] S. J. S. M. D. a. P. H. Rees, "Qualitative Comparison of North American and U.K. Cooling Load Calculation Methods.," *International Journal of Heating, Ventilating, Air-Conditioning and Refrigeration Research*, vol. 6, pp. 75-99, 2000.
- [3] J. D. Spitler, "Load Calculations Applications Manual (I-P)," ASHRAE, [Online]. Available: <https://www.ashrae.org/File%20Library/Technical%20Resources/Bookstore/preview-load-calculations.pdf>.
- [4] M. A. F. a. M. Bahrami, "<https://www.sae.org>," [Online]. Available: <https://www.sae.org/publications/technical-papers/content/2013-01-1507/>.
- [5] Asyraei, "ashraei fundamental table 1 chapter 5?".
- [6] S. S. F. T. T. C. K. S. A. P. a. D. M. Tyler Hoyt, "CBE Thermal Comfort Tool. Center for the Built Environment," Center for the Built Environment University of California Berkeley, 2019. [Online]. Available: <https://comfort.cbe.berkeley.edu/EN>.
- [7] I. O. f. Standardization, "ISO 6946:2007—Building Components and Building Elements—Thermal Resistance and Thermal Transmittance—Calculation Method," Geneva, Switzerland, 2007.
- [8] I. O. f. Standardization, "ISO 9869-1:2014—Thermal Insulation—Building Elements—In Situ Measurement of Thermal Resistance and Thermal Transmittance. Part 1: Heat Flow Meter Method," Geneva, Switzerland, 2014.
- [9] R. Albatici and A. Tonelli, "Infrared thermovision technique for the assessment of thermal transmittance value of opaque building elements on site.," *Energy Build*, 2010.
- [10] E. s. m. Eriksson Johansson, "Mster thesis: Interior climate simulation of electric buses," Chalmers University, Gothenburg, 2019.
- [11] G.-S. Tutorials, "Gamma Technologies," Gamma Technologies, 2020.
- [12] M. F. Ashby, *Materials Selection in Mechanical Design*, Oxford: Elsevier Ltd., 2017.
- [13] Y. A. Cengel, *Heat Transfer: A Practical Approach*, New York: McGraw-Hill, 2002.
- [14] I. A. J. U. Amaya Martinez-Gracia, in *SOLAR HYDROGEN PRODUCTION processes, systems and technologies*, 2019, pp. 113-149.